INTERFACIAL AREA

INTERFACIAL AREA MEASUREMENT USING A RADIOISOTOPE TECHNIQUE

By

ALBERT MIRZA KHACHADOUR, B.Eng. (Hons.)

A Thesis

Submitted to the School of Graduate Studies

in Partial Fulfilment of the Requirements

for the Degree

Master of Engineering

(PART A)

McMaster University

April, 1979

MASTER OF ENGINEERING (1979)
(Engineering Physics)

McMASTER UNIVERSITY
Hamilton, Ontario

TITLE: Interfacial Area Measurement Using a Radioisotope Technique

AUTHOR: Albert Mirza Khachadour, B.Eng. (Hons.) (Liverpool University)

SUPERVISOR: Professor S. Banerjee

NUMBER OF PAGES: vii, 76

ABSTRACT

A radioactive technique to determine interfacial area between solid-liquid and liquid-liquid phases has been investigated. Plastic and liquid scintillators and β-particles from tritium solution were used for this purpose.

The tritium β-particles have a very short range (about 5 μm in water), and the surface area of contact between the tritium bearing fluid and the scintillator bearing phase is expected to be proportional to the scintillation count rate, which in turn is proportional to the number of betas crossing the interface from a very thin region.

To test this hypothesis, two phases were placed together in a cylindrical plexiglas container, which in turn was placed in an aluminum light-tight housing. The housing also enclosed the photo-multiplier tube (PMT). Pulses corresponding to scintillations due to β absorption were taken from the PMT and fed to a suitable electronic circuit. The count rate was obtained with a multi-channel analyser.

It was found that the count rate is a linear function of interfacial area between the tritium bearing fluid and the scintillating material. Some deviation from linearity was however noticed at very low tritium concentration. The count rate remained the same for a given interfacial area regardless of orientation of the surface(s) with respect to the photocathode face.

This appeared to confirm the hypothesis that interfacial area could be measured in systems of this type by measuring the scintillation count rate.

ACKNOWLEDGEMENT

I would like to express my sincere thanks and gratitude to Professor S. Banerjee for his invaluable guidance and constant encouragement throughout this work. Thanks are also due to Dr. J. Harvey and his assistants in the Health Physics Department for their help in carrying out the experiment in the high level laboratory, and for many useful discussions. I would like also to thank my collegues in the Nuclear Research Building for their help in loaning equipment and setting it up. Finally, I would like to extend my appreciation to the Engineering Physics Department of McMaster University for both accepting me as a graduate student and providing me with this unique opportunity of working towards my degree.

TABLE OF CONTENTS

LIST OF FIGURES

1. INTRODUCTION

In a two-phase system such as when a gas forms a dispersion in a liquid, knowledge of interfacial area is required for system analysis. For example, in the analysis of mass transfer between two phases if the interfacial area can be estimated, then the corresponding mass transfer rate can be calculated. Interphase mass transfer is of great importance in many industrial operations, such as organic oxidations, chlorinations and other fast reactions. Interfacial areas are also of importance in determining the interphase transfer of mass, momentum and energy in steady and transient two-phase flow.

Several investigations to determine interfacial areas in bubble column and stirred vessel have been reported in the chemical engineering literature. These have led to correlations relating interfacial area to system variables such as flow rates, densities, etc. Due to the lack of good hydrodynamic models, the relevant variables are not completely identified and their effect is not well understood. The various factors affecting overall transfer in fluid-fluid dispersions have been reviewed by Sideman et al. [1] and Valentin [2].

Various methods are available for measuring interfacial areas in gas-liquid and liquid-liquid systems. The most widely used methods are either chemically based or optically based.

In the chemical method, the interfacial areas are determined by measuring the rates of absorption of a gas that undergoes chemical reaction with a component of the liquid phase. The reaction kinetics

must be well understood. The theory of the available methods for the measurement of interfacial area, gas and liquid side mass transfer coefficient has been discussed in a survey by Sharma and Danckwerts [3]. In their paper they also discussed the types of chemical systems useful for such measurement in gas-liquid and liquid-liquid systems. Shilimkan and Stepanek [4] have measured the interfacial area for the case of cocurrent gas-liquid upward flow in tubes 10, 15 and 20 mm inside diameter, using the technique of absorption with fast chemical reaction of carbon dioxide into 1 N aqueous solution of sodium hydroxide. The interfacial area showed a maximum at a different superficial velocity for different tubes. Their work was a continuation to the work done previously by Kasturi and Stepanek [5], who investigated separately the interfacial area and liquid and gas side mass transfer coefficients in a rather narrow tube. Their work was carried out for the case of cocurrent gas-liquid flow through a vertical tube 6 mm i.d., by absorbing sulpher dioxide into sodium hydroxide solution and sulpher dioxide into sodium carbonate-sodium bicarbonate solution respectively. A model based on the analogy between momentum and mass transfer has been proposed by them for the rate of mass transfer in the liquid phase. A correlation in terms of dimensionless groups was presented for the gas side mass transfer coefficient.

Sridharan and Sharma [6] discussed new systems developed for the measurement of effective interfacial area by the chemical method, which allow the use of hydrocarbon solvent, such as toluene, xylene etc. polar solvent, such as benzyl alcohol, cychohexanol, etc, and highly viscous solvents such as diethylene glycol, polyethylene glycol etc.

In all the above cases, the reaction between carbon dioxide and selected amines was employed. Effective interfacial area and liquid mass transfer coefficient have been measured by the absorption of carbon dioxide and pure carbon monoxide/propylene respectively into cuprousamine solutions. Metha and Sharma [7] used absorption with slow chemical reaction to find the liquid-side mass transfer coefficient. Several systems were used for this purpose, for example carbon dioxide diluted with air was absorbed in sodium carbonate-bicarbonate buffers, oxygen in air was absorbed in acidic and neutral solutions of cuprous chloride, etc.

Although the chemical method provides an elegant technique to determine interfacial areas, it has the disadvantage that a systematic investigation of liquid phase properties, such as viscosity and interfacial tension, on the interfacial area is very difficult, since the addition of surface active or viscous components would make a new and time consuming investigation of the kinetics of the chemical reaction necessary. The oxidation of sodium sulphite solutions has also been widely used to illustrate the method, see Westerterp et al. [8] and Linek and Mayrhoferova [9].

In optically based methods, three techniques have been used in measuring interfacial areas, namely; light scattering or transmission, light reflection and photography.

Light scattering is the most widely used technique in this category. It is based on the light scattering properties of gas bubbles in liquids. The principle is that a parallel light is passed through the dispersion and a photocell is placed at some distance from it. Only the part of the beam which does not meet any obstacle i.e. gas

bubble, is detected by the photocell. The technique has been used by Vermeulen et al. [10], Calderbank [11] and McLoughlin and Rushton [12]. Calderbank [11] has shown the theory for the attenuation of a light beam passing through a dispersion and derived the relationship

$$\ell n\ I_o/I = SL/4 \qquad (1)$$

where I_o and I are incident and transmitted light intensities respectively, S interfacial area per unit volume of dispersion and L the optical path length.

This formula has been used by many other workers. McLoughlin and Rushton [12] and Curl [13] have shown that the bubble size distribution does not affect the fraction of light transmitted by a dispersion, and that the fraction of light transmitted is directly related only to the interfacial area and the path length. This statement leads to the same equation (1) above.

Lee and Meyrick [14] found that the minimum value of (I_o/I), the ratio of incident to transmitted light intensity, which can be measured with reasonable accuracy and reliability is about 100. This means that the above relationship holds up to $SL < 20$. Above this value multiple scattering becomes important. Assuming a minimum path length of 3 cm, which seems to be a reasonable requirement, it follows that the maximum interfacial area which can be measured with this method is about 700 m^2/m^3. Landau et al. [15] reported values of interfacial areas up to 600 m^2/m^3. They have also found that this technique could be used with confidence for bubbles down to 100 μm diameter.

The above limitation (SL < 20), has evidently prevented the widespread use of this technique. Recently, however, ways of overcoming this problem have been suggested by Landau et al. [15]. It has also been suggested to decrease the path length to 1 cm, compared to about 50 cm used by Calderbank [11]. There has also been a proposal for a new correlation essentially similar to Calderbank's correlation, but applicable to a wide range of velocity, pressure and temperature.

The second technique in this category is light reflection. It is not widely used because it is only suitable for measurements of interfacial area near vessel walls and therefore is not applicable for the measurements of integral values of interfacial area in vessels with large local variations of interfacial area, Calderbank et al. [16].

The photographic technique has been used by several workers by taking photographs of the liquid contents of the reactor through a transparent vessel wall or with an intrascope in the interior of the reactor, Van Dierendonck et al. [17] and Towell et al. [18]. In another case, Kawecki et al. [19] extracted bubbles from the reactor by means of a tube connected to a small, square-section volumn. The bubbles in the column were photographed. The latter technique was also used by Brown and Craddock [20].

The specific interfacial area S, was calculated from the following relationship

$$S = 6(1-\varepsilon)/d \qquad (2)$$

where $(1-\varepsilon)$ is gas hold up and d is bubble diameter.

There are two serious limitations of both photographic measuring techniques. The first, is that only local samples can be taken, and second the hydrodynamic behaviour of the dispersion at the sampling point is disturbed. Kawecki et al. [19] measured with their method interfacial areas up to 800 m^2/m^3 with bubbles of 25 mm diameter in pure water.

It has been observed that the chemical and physical methods yield different values of interfacial area measured under identical geometrical, physical and operational conditions. Only in very few cases the same values of interfacial area were measured in identical systems with different measuring techniques. Reith and Beek [21] compared the chemical method and the photographic method in bubble columns. Excellent agreement was obtained. A comparison between these techniques for determining interfacial areas in gas-liquid dispersions in stirred tanks and bubble columns reported by several authors is given by Reith [22]. Sridhar and Potter [23] also compared the light transmission and chemical methods for measuring interfacial areas in agitated vessels. They have found that the latter yields constantly higher values of interfacial areas. They suggest that the criteria for the rate to be independent of hydrodynamics may fail when the mass transfer coefficients vary widely and that while the chemical method is suitable for bubble columns it is possibly unreliable when applied to contactors where high local shear rates exist.

Both the chemical and optically based methods have limitations and are not reliable in all flow regimes. It was therefore of interest to investigate a more direct method of measuring interfacial area. The

basic principle is simple. If a radioisotope with very short range radiation is present in one phase, and a scintillating material in the other, then the number of radiation particles crossing the interface will be dependent on a very thin region near the interface. Furthermore, the radiation will be absorbed within a very short distance in the scintillating phase. Thus, the number of scintillations can be expected to be proportional to the volume of the fluid very near the interface and hence to the interfacial area. The work reported in this thesis tests this hypothesis.

2. THEORETICAL CONSIDERATIONS

2.1 Scintillators and β-Particles

When some materials are exposed to ionizing radiation, such as x-rays, α, β, γ or neutron radiations, they emit visible light flashes or "scintillations". These scintillations can be detected with a photomultiplier tube (PMT), and converted into electrical pulses which can be measured with a suitable electronic system. A considerable literature exists on scintillation systems concerning different aspects and applications. Some of these are given in references [24-29].

A wide variety of scintillators is in use today. These can be divided into organic and inorganic, and may exist in the form of crystals, liquids, solids or gases. Although all scintillator types are sensitive to β-rays to varying degrees, the organic materials are most widely used for detecting these particles. Good organic scintillators combine high light yield with high transparancy and have lower backscattering than inorganic scintillators containing high Z elements. Also, the fast response of the organic scintillators, coupled with the availability in liquid and solid solutions as well as crystalline forms, contributes greatly to their utility.

The good liquid and plastic scintillators are not chemically pure liquids or plastics but liquid or solid solutions of organic scintillators in different solvents. The light yields of pure liquids and plastics seldom reach 10% of the light yeild of anthracene, (which has the highest light output for a pure crystal), and are generally

below 3 or 4% especially in the case of organic liquids [26]. Therefore, quantities of special solutes are dissolved in these liquids, to obtain higher intrinsic efficiencies, (defined as ratio of the light energy generated in the scintillator to the kinetic energy spent by the charged particles). Some types of scintillators and their properties are shown in Table 1. All are organic scintillators except for NaI(Tℓ) which is inorganic.

β-particles of a given energy lose almost equal fractions of their energy in passing through thin layers of different materials, provided that the layers have equal mass per unit area or more precisely, equal numbers of atomic electrons per unit area. For most scintillators the intrinsic efficiency for the conversion of absorbed energy into light energy is nearly energy-independent (within ±10% for β-particles above 1 KeV [26]). The relative response of a scintillation detector to electrons of various energy is strongly dependent on the thickness of the scintillator. If the thickness is very small in comparison to the range of all electrons under consideration, the electrons lose only a small fraction of their energy in the scintillator. On the other hand, in a scintillator the thickness of which exceeds the ranges of all β-particles under consideration, all betas not scattered back through the entrance surface are completely stopped. The energy transfer to such a "thick" scintillator is therefore a nearly linear function of the total beta energy.

The attenuation of β-rays in matter in some ways is more complicated than for heavy charged particles. The reasons being that β-rays are emitted in a continuous energy spectrum and are strongly

TABLE 1: Properties of Some Scintillators

Scintillator	Type	Specific Density	Wavelength of max. emission, nm	Refractive Index	Light yield % anthracene	Decay time constant, nsec.
Anthracene	Crytal	1.25	447	1.62	100	30
Stilbene	Crystal	1.16	410	1.626	50	4.5
NaI(Tℓ)	Crystal	3.67	413	1.775	230	230
Pilot B	Plastic	1.032	408	1.58	68	1.8
NE-224	Liquid	0.877	425	1.505	80	2.6
NE-213	Liquid	0.874	425	1.508	78	3.7

deflected in each encounter with an atom, being less massive particles. As a result, β-rays move in a complicated zigzag paths and not in straight lines. Nevertheless, it has been found experimentally that the specific ionization of a beam of β-rays varies approximately with distance into an absorber [30] as

$$I = I_o e^{-\mu_\ell x} \tag{3}$$

where I, I_o are transmitted and incident radiation intensities respectively, μ_ℓ is the linear attenuation coefficient of the absorber, measured in cm^{-1}, and x is the thickness of the absorber in cm. Sometimes equation (3) is expressed in terms of mass attenuation coefficient, μ_m then

$$I = I_o e^{-\mu_m x_m}$$

where μ_m is in cm^2/gm and x_m is in gm/cm^2. It should be noted that $\mu_m = \mu_\ell/\rho$ where ρ is the density of the absorber in gm/cm^3.

A more useful parameter related to the attenuation of β-rays is the maximum range, R_m. This is defined as the thickness of absorber required to stop the most energetic of the electrons. Theoretical expressions for the rate of energy loss in an absorber are very complicated, Heitler [31] showed that the energy lost per cm. path by a particle is given by

$$\left(-\frac{dE}{dx}\right)_{coll} = \frac{3}{4} NZ\phi\mu \left(\frac{z}{k}\right)^2 \left[\log \frac{2\mu k^2 W_m}{(IZ)^2(1-k^2)} - 2k^2\right] \tag{4}$$

where E=total energy of the particle

x = path length

N = number of atoms per cm^3

ϕ = universal cross-section

$= \frac{8\pi r_o^2}{3}$ where r_o is radius of electron

μ = rest energy of electron, $(m_o c^2)$

z = charge of primary particle

Z = atomic number

I = average ionization energy

k = ratio of particle velocity to that of light, $(k = \frac{v}{c})$

W_m = maximum energy that can be transferred to a free electron by the primary

A theoretical range can be defined from the theoretical rate of energy loss formula (4). A fast particle traversing matter has a more or less well defined range only when it loses energy steadily and the fluctuations of energy loss in a definite length of path are small. This is the case for the energy loss by collisions but not for that by radiation. Since the total energy loss per cm of path is the sum of radiation and collision losses, it will be convenient to define an average range, the distance which the particle would travel if it always suffered just the average energy loss due to radiation and collisions. This average range is then given by

$$R_t = \int_{\mu}^{E_o} dE\left(-\frac{dE}{dx}\right)^{-1} \qquad (5)$$

where R_t represents theoretical average range, E_o is initial energy and μ is energy of β-particle at rest.

In practice this cannot be carried out for the full range of the particle because of the corrections necessary to the explicit formula for dE/dx at low energies. Range-energy curves are therefore constructed semi-empirically by combining observations of the range of particles of known energy with integrations of the energy-loss formula over some particular region.

The difficulty in solving the above differential equation is obvious. Therefore, various simpler approximate expressions for this relation between the range and energy have been given by a number of authors. An excellent review of this subject is reported by Katz and Penfold [32]. One of the earliest suggestions was an equation of the following form

$$R_m = AE_m - B \tag{6}$$

where E_m is maximum beta energy and R_m is maximum range.

Since then there have been many values suggested for A and B [32]. However, the relation between the energy and the range does not appear to be exactly linear in the region of energy concerned, therefore these values can only be regarded as approximate. For low energy intervals the following equation was suggested

$$E_m = 1.92(R_m^2 + 0.22R_m)^{1/2} \tag{7}$$

A number of authors have proposed a relation between range and energy of the form $R_m = aE_m^n$, where 'a' and 'n' are constants. Different values were suggested for these constants by several authors. Katz and Penfold [32] have let 'n' be variable and have used the equation

$$R_m = aE_m^{(b-c\ \ell n\ E_m)} = aE_m^n \tag{8}$$

b and c being constants. From their experimental data they have found that

$$n = 1.265 - 0.094\ \ell n\ E_m$$

Their final equation for the energy-range relation was

$$R_m = 0.412E_m^{(1.265-0.094\ \ell n\ E_m)} \tag{9}$$

where the energy is expressed in MeV and R_m in gm/cm^2.

The above empirical formula (9) is valid for energies less than 2.5 MeV. For energies greater than this value and up to 20 MeV they suggested a relation similar to equation (6), thus

$$R_m = 0.530\ E_m - 0.106 \tag{10}$$

The maximum range of β-prticles from any radioisotope in a material can thus be determined using one of the above relationships, depending on the maximum energy emitted. For example, the maximum range of β-particles from tritium (E_m = 18 keV), in the plastic scintillator "Pilot B" will be about 5.3 μm and in the liquid scintillator "NE 224" approximately 6.3 μm, using equation (9) above. These values are in good agreement with manufacturer data which give approximate value of 5 μm for electron range in "Pilot B". Also, Evans [33] reported that β-rays from tritium can be stopped by about 6 μm of material of unit density, such as water. All these figures indicate that a very small thickness of scintillators will stop all β-particles

from a tritium source.

Thus, it can be assumed that β-rays crossing an interface between tritium bearing and scintillating phases will originate from and be absorbed within a very short distance of the interface. Hence the light-emitted may be expected to be proportional to the interfacial area. This hypothesis is supported by the results reported by Blincow and Webster [34] who investigated attenuation coefficients of different plastic scintillators and found that they vary with scintillator diameter, or in other words with interfacial area.

2.2 Light Collection from Scintillation Process

The absorption of energy by a substance and its re-emission as visible or near-visible radiation are known as luminescence. In the luminescence process the initial excitation can come from many origins. Several of these are light, mechanical strains, chemical reaction and heating. The scintillation accompanying nuclear radiation has its origin in the excitation and ionization produced in the substance by radiation.

If there are allowed transitions between the resulting excited state or states and the undisturbed state of the material, the de-excitation accompanied by light emission occurs in about 10^{-8} sec. or less, which is the order of the lifetime of an atomic state for an allowed transition. Only those scintillators with the shorter durations are useful for the detection of nuclear radiation.

To a first approximation, the number of light photons n_p emitted in the time t after the arrival of the ionizing particle can

usually be represented by the simple exponential growth law [25]

$$n_p = n_{p\infty}(1-e^{-t/\tau}) \tag{11}$$

where $n_{p\infty}$ is the total number of light photons. The time τ required for the emission of the fraction $(1-e^{-1})$, or 63% of the photons, is referred to as the "decay time".

Most of energy of excitation and ionization produced in the scintillation by the nuclear radiation is quickly degraded into heat with only a small percentage of it escaping as visible or ultraviolet radiation. The fraction converted into light energy for scintillators in common use varies from a fraction of a percent to around 40%. The loss of light depends on the properties of scintillators and the emitted radiation itself.

The light output incident on the photocathode of the PMT depends on various physical constants of the scintillating material, such as cross-sections for absorption of primary radiation, (which vary strongly as a function of the energy of the primary radiation hence influencing the overall detection efficiency), the intrinsic efficiency of the scintillator etc., and is strongly influenced by geometrical and optical features of the system, such as reflectors and light pipes. Other properties affecting the light output are transparency and the index of refraction of the scintillator.

High transparency of scintillating material for the emitted light is always desirable, but it is not necessary to the same extent for the detection of various types of radiation. A relatively poor transparency may still be sufficient if the incident radiation has low

penetration into the scintillator, which can therefore be made thin.

The index of refraction determines the critical angle for total reflection at the surface of the scintillator. An index of refraction much higher than that of glass causes considerable losses by multiple internal reflection and eventual absorption.

The scintillator should be as close to the photocathode as possible and should be surrounded by a reflecting light shield. Aluminum foil is often used for this purpose. The efficiency seems to be better if the foil is not in contact with the scintillator, because optical contact may impair total reflection at the surface.

The principle of light piping by means of transparent rods or hollow metal pipes utilizes the repeated total reflections at the surface of the pipe and keeps the light loss within tolerable limits. Lucite, plexiglas, glass and quartz have been used as transparent pipe materials.

For several reasons such as space limitations and ambient conditions, it may be desirable to place the scintillator at a distance from the PMT. Several feet of light pipe has been used with success [35]. Gradual bends in light pipes can be made without appreciable light loss.

In the experimental arrangements of this work (see Figs. 13 and 14), weak β-particles from tritium source have the advantage that their penetration into the plastic scintillator is very minute, thus permitting the remainder of the scintillator to function only as a light pipe. Most of the light incident on aluminum wall surrounding the sample will

be reflected. For wavelength regions (400-500) nm about 90% of normal light incident on aluminum will be reflected back [36]. Therefore, for each sample setting a relatively constant fraction of the light emitted will be detected by the photocathode. This light fraction will be proportional to the area of the aluminum disc opening, hence to interfacial area of the two phases.

3. EXPERIMENTAL ASPECTS

3.1 Experimental Equipment

Most of the work done in these tests was with commercial Pilot B plastic scintillator, which is a polyvinyl-toluene, host containing poly-terphenyl and dyphenyl-stilbene. Some tests with liquid scintillators NE224 and NE213 were also carried out. The source of radiation was aqueous tritium solution which emits weak β-particles of maximum energy 18 keV.

Discs of 2-3 mm thick were cut from a scintillator rod 25 mm diameter and prepared for the experiments. Manufacturer recommendations for preparing these discs were closely followed. After lathe-cutting of the discs, they were sanded by rubbing at right angle using #240 grade silicon carbide waterproof polishing paper with water. This was followed by polishing with #400 grade, then #600 grade. In each instance sanding was done at right angles to the previous operation. Final polishing was done using polishing alumina, particle size 5 microns, slightly moistened with a little water on flannel polishing cloth, using a slow speed rotating wheel.

The source and the scintillator disc were place together in a cylindrical container made of plexiglas. This in turn was placed in a light-tight aluminum housing where the counting was done. The housing consisted of two main detachable parts, see Fig. 1. In one part, the photomultiplier tube (PMT) of type XP-1000 was fixed using 'O' ring supporters, and the second part contained a chamber well where the samples were placed for counting. The diameter of the well

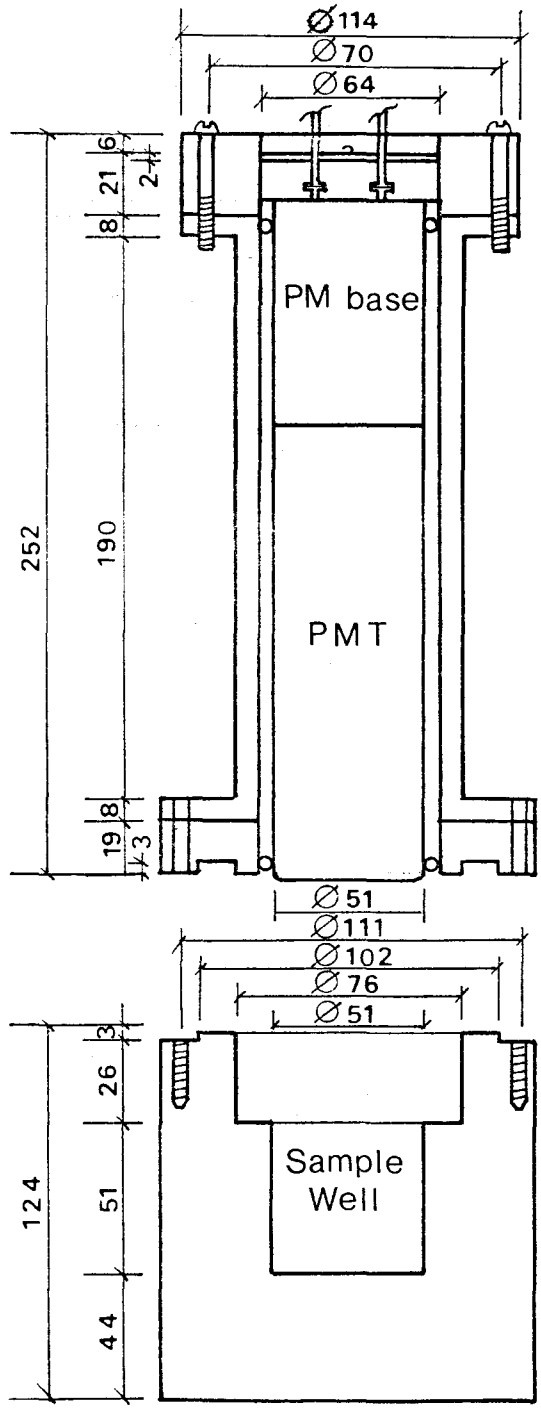

Measurements in mm

FIG.1. THE LIGHT-TIGHT HOUSING ARRANGEMENT WITH PMT (A LONGITUDINAL VIEW)

was the same as the plexiglas container outside diameter, and this in turn had an inside diameter approximately that of scintillator disc. This ensured that the same part of the photocathode would be exposed to the light from the scintillators for the entire experiments. The inside of the housing was painted flat black except the well portion in order to eliminate reflection.

A block diagram of the system used in these tests is shown in Fig. 2. The PMT was supplied with a high voltage of 1200 volts. The pulses from the PMT were fed to pre-amplifier, amplifier then to the multi-channel analyzer (MCA), type TN-1705.

Some preliminary tests were carried out in order to get the best knob settings on MCA to cut back the noises from PMT, since cooling of PMT was not employed. Several sets of background and sample readings were viewed on the cathode-ray tube (CRT) screen of the MCA. Comparing the background count spectrum to that of the sample it was noticed that most of the noise fell below channel 150. A typical spectrum of background and a sample spectrum is shown in Fig. 3. Therefore, in actual tests, counts above channel 150 and up to channel 1000 were integrated and recorded. There was no need to go beyond channel 1000, because the count rate dropped to background count well before reaching this channel.

3.2 Experimental Procedure

The general procedure for the tests was as follows. Samples of aqueous tritium solution and scintillators were placed in the plexiglas

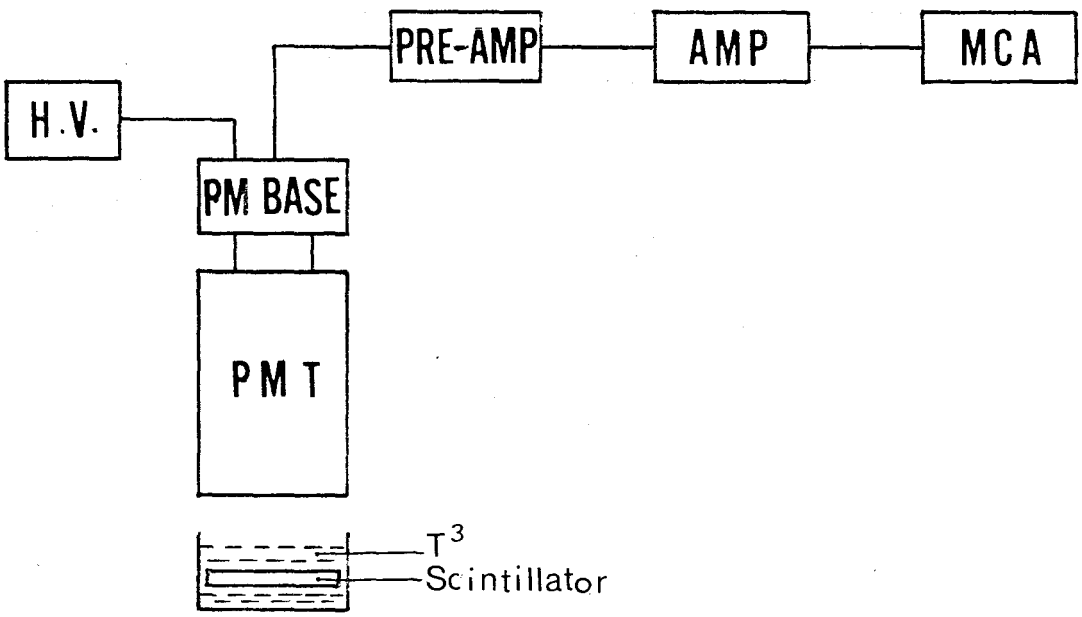

FIG. 2. BLOCK DIAGRAM OF EXPERIMENTAL SET-UP

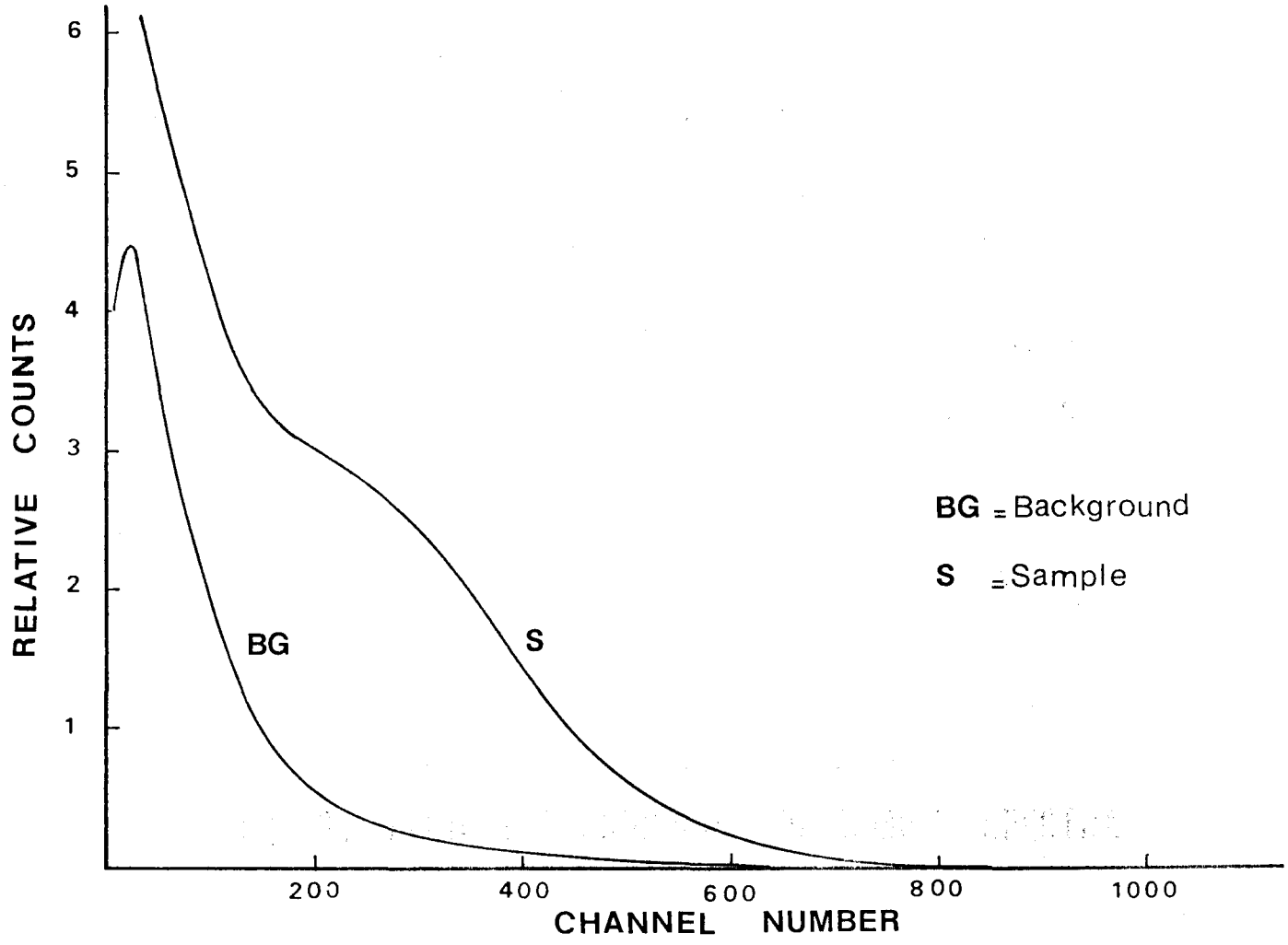

FIG. 3. TYPICAL BACKGROUD AND SAMPLE SPECTRA

container, and then positioned in the chamber well of the aluminum housing. The surface area of scintillators was varied by means of aluminum discs 3 mm thick, having different diameter holes in their centres, placed above the container. After each sample counting, the aluminum disc was replaced and counting was repeated. Each sample was counted for 60 seconds, and at least five readings were taken for each sample.

After each sample reading, it was necessary to disconnect the aluminum housing for the next sample counting. Therefore precautions were taken not to expose the photocathode to direct light by placing a rubber cover on it. Otherwise, when the PMT is exposed to room light, it results in trapping of energy in the photocathode when the tube is placed in the dark and the high voltage is applied, this effect will manifest as an excessive dark current. After 24 hours or so in dark, the dark current should fall to its equilibrium value. All new readings were taken after five minutes from applying the high voltage to the system, so that a steady-state of the electronic equipment was maintained. It was also insured that geometrical configuration for the counting was not altered from sample to another, so that always the same area of the photocathode was exposed to the samples.

In plastic scintillator tests, when determining interfacial area, only the two faces of a disc were considered. Circumferential area, due to thickness of the disc, was neglected. The error thus introduced is small, as shown in Appendix A32.

3.3 Test Matrix

Tests were first carried out with the plastic scintillator. Tritium was obtained from a bottle containing a high activity solution (1 Ci/100 ml), and diluted with distilled water to desired values. The source solution covered the scintillator disc(s) completely.

Test 1:

This test was run to see the variation of counting rate with specific activity at constant volume. Ten samples of different activities ranging from 0.5 mCi/2nd to 20 mCi/ml were prepared for this purpose. A single plastic disc was used in this test. Readings of count rate were taken for each sample. A graph of specific activity versus count rate were plotted.

Test 2:

In this test a single disc was also used with various source activities. Three different activities viz. 0.5, 6 and 8 mCi were used. In each case a graph of interfacial area versus count rate was plotted.

Test 3:

In this test readings were taken when more than one plastic scintillator was used. With the housing in a vertical position, the plastic scintillators were placed one on top of the other, one at a time and counted for each case. The plastic scintillator discs were hold in a thin plexiglas rings, having very short legs, which kept them apart about 3 mm. Four such discs were used and the count rates were recorded for 1, 2, 3 and 4 discs. To see if the orientation of the discs affected the counting rate, the test was repeated with the discs

rotated 90 degrees from their previous positions.

Test 4:

A test with two plastic scintillator discs was carried out by varying the distance between the discs, to see whether the separation had any effect on count rate. The separation was varied from 0.5 mm to 3 mm.

Test 5:

Some tests with liquid scintillators were also carried out. First, a single plexiglas container was used with 2 ml tritium solution of specific activity 5 mCi/ml, covered with 1 ml of liquid scintillator NE224. The same procedure used for the plastic scintillator was used here.

Then, four cylindrical plexiglas containers were machined. These had approximately equal volumes (4.5 ml), but different diameters, with very thin wall thicknesses. To each of these containers, 2 ml of tritium solution, specific activity 2 mCi/ml was introduced. On top of tritium an equal thickness (3 mm) of the liquid scintillator was added. Readings were taken for each container in two positions. First, with the axes of container and PMT in the same line, and then with these axes at right angles to each other. All the results were tabulated and plotted.

Test 6:

A series of tests with liquid scintillators and plastic scintillator was carried out, to observe the effect of scintillator thickness on count rate.

A first run was done with the plastic scintillator. A constant

volume of tritium solution, specific activity 6 mCi/2 ml was used in one of the plexiglas containers. The thickness of the scintillator was varied from 2 mm to 10.5 mm, and the count rate in each case was recorded.

A similar test was carried out with the two available liquid scintillators. Results were recorded for four different thicknesses in each case.

Another run was done with the liquid scintillator NE224, using inactive distilled water. Count rates for three different thicknesses of the scintillator were recorded.

Test 7:

This test was carried out to see the time effect on a liquid scintillator sample.2 ml inactive distilled water was introduced in a container (25.4 mm i.d.) and a small amount of liquid scintillator NE224 was added on top of it, so that the thickness of the scintillator was 3 mm. The sample was counted every hour. Seven sets of readings were taken.

The same test was repeated with tritium solution replacing the inactive distilled water.

4. RESULTS AND DISCUSSIONS

The variation of light intensity (count-rate) from the scintillator disc is shown as a function of specific activity for a constant volume of tritium bearing liquid and scintillator in Fig. 4. It can be seen that a linear relationship exists between the two parameters. This graph was used afterwards to make the necessary corrections, when the specific activity varied from one test to another, Table A1.1.

Figs. 5, 6 and 7 show variation of count rate versus interfacial area of the plastic scintillator. It was observed that a slight deviation from linearity exists at small surface area in case of low specific activity, namely 0.5 mCi/2 ml. However, in the other two cases this phenomenon was not noticed, Table A1.2.

Figs. 8-11 show the count rate as a function of interfacial area, when more than one plastic scintillator was used. In this test a larger volume container was used so that it could accommodate four scintillator discs. Data for these runs are shown in Table A1.3(I). As can be seen from the graphs, linearity was not affected when several scintillators were used. The above arrangement of the discs is analogous to the case of water bubbles in a two-phase flow, when several of these bubbles are in the same line. A schematic diagram of this arrangement is shown in Fig. 13.

Results of these multiple-disc tests were redrawn on a single graph Fig. 12, which indicates the linear character of the relationship between interfacial area and count rate, irrespective the number

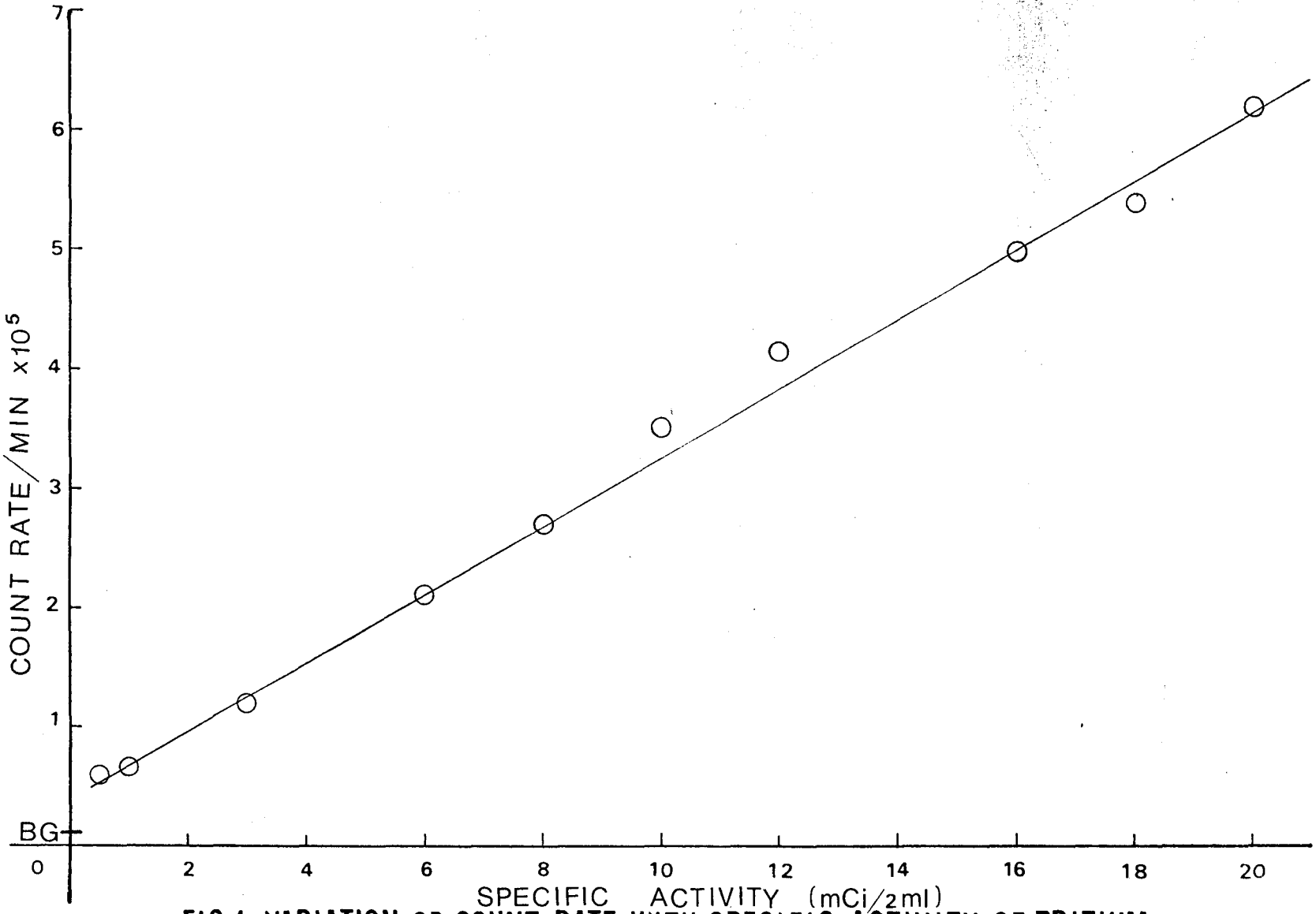

FIG.4. VARIATION OF COUNT RATE WITH SPECIFIC ACTIVITY OF TRITIUM

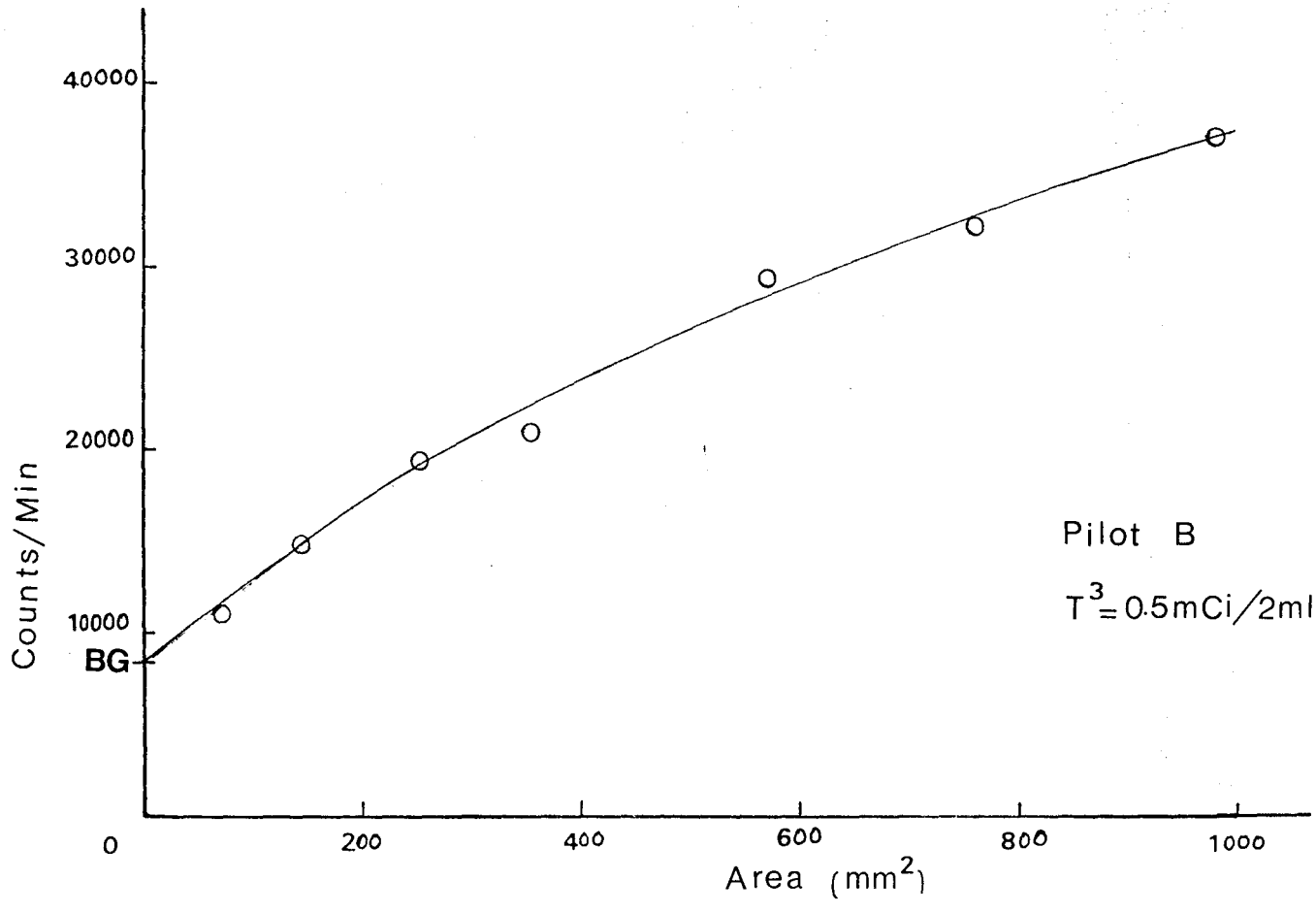

FIG.5. RESPONSE OF COUNT RATE TO INTERFACIAL AREA USING 0·5mCi/2ml T^3

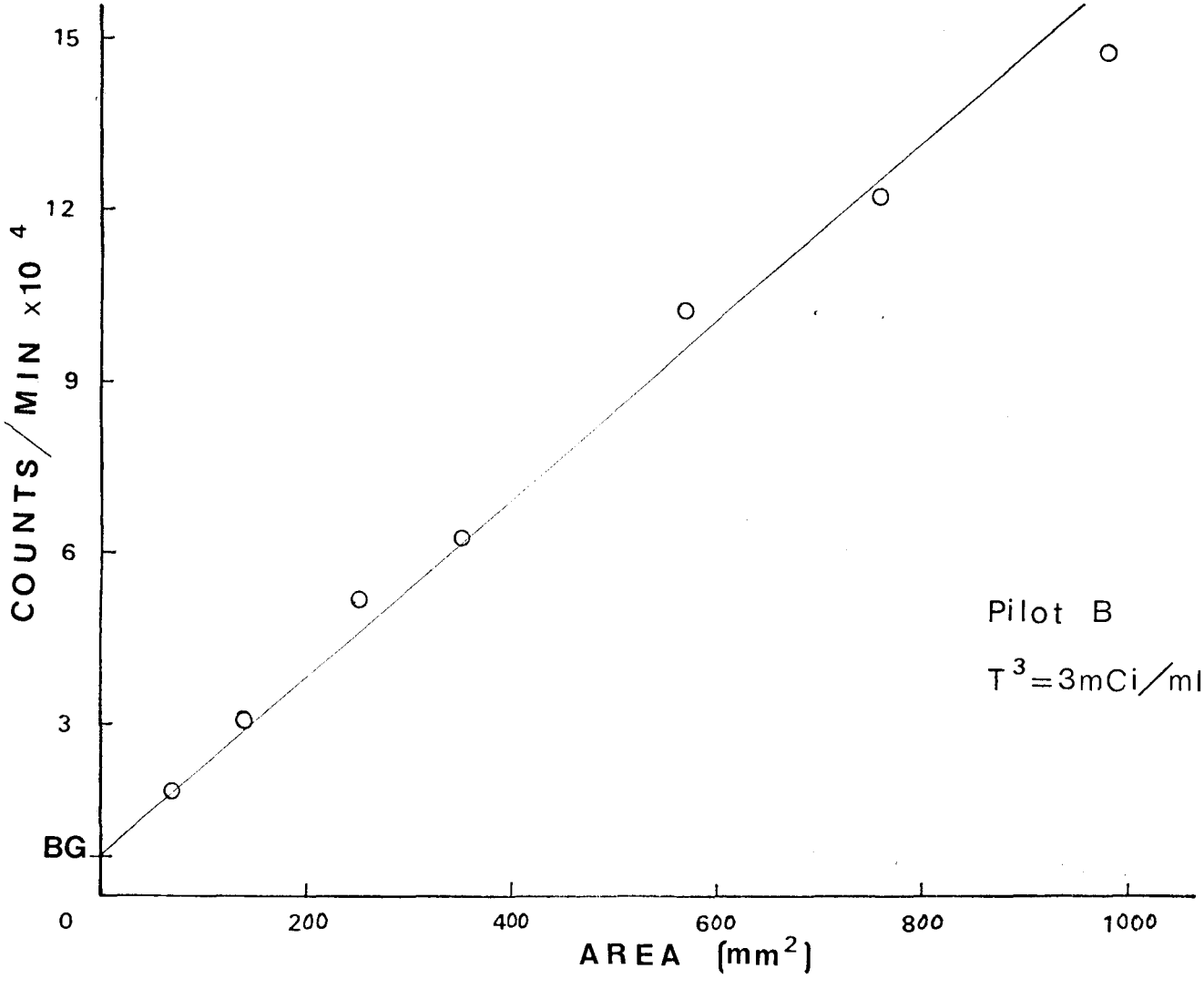

FIG.6. RESPONSE OF COUNT RATE TO INTERFACIAL AREA

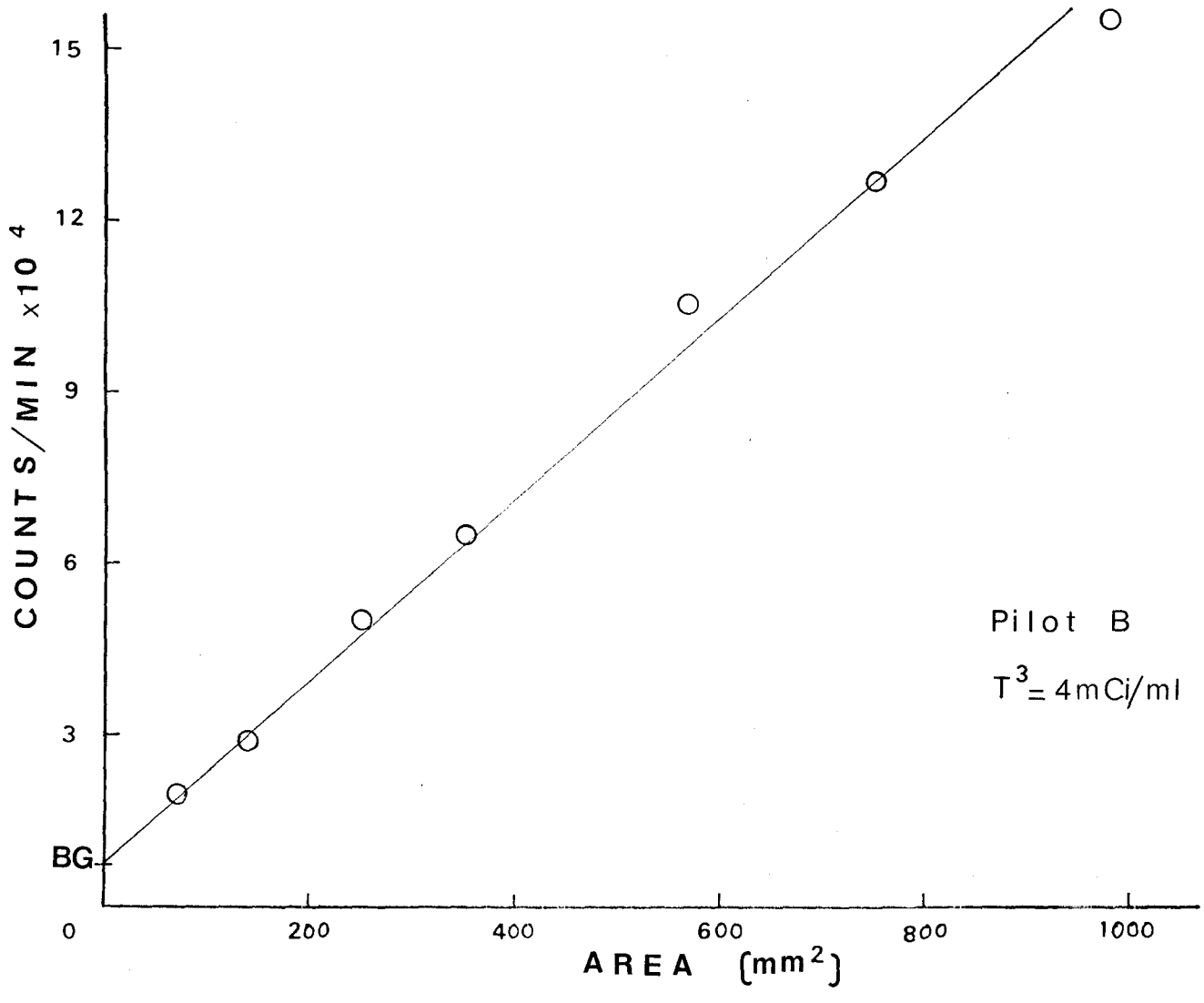

FIG. 7. RESPONSE OF COUNT RATE TO INTERFACIAL AREA

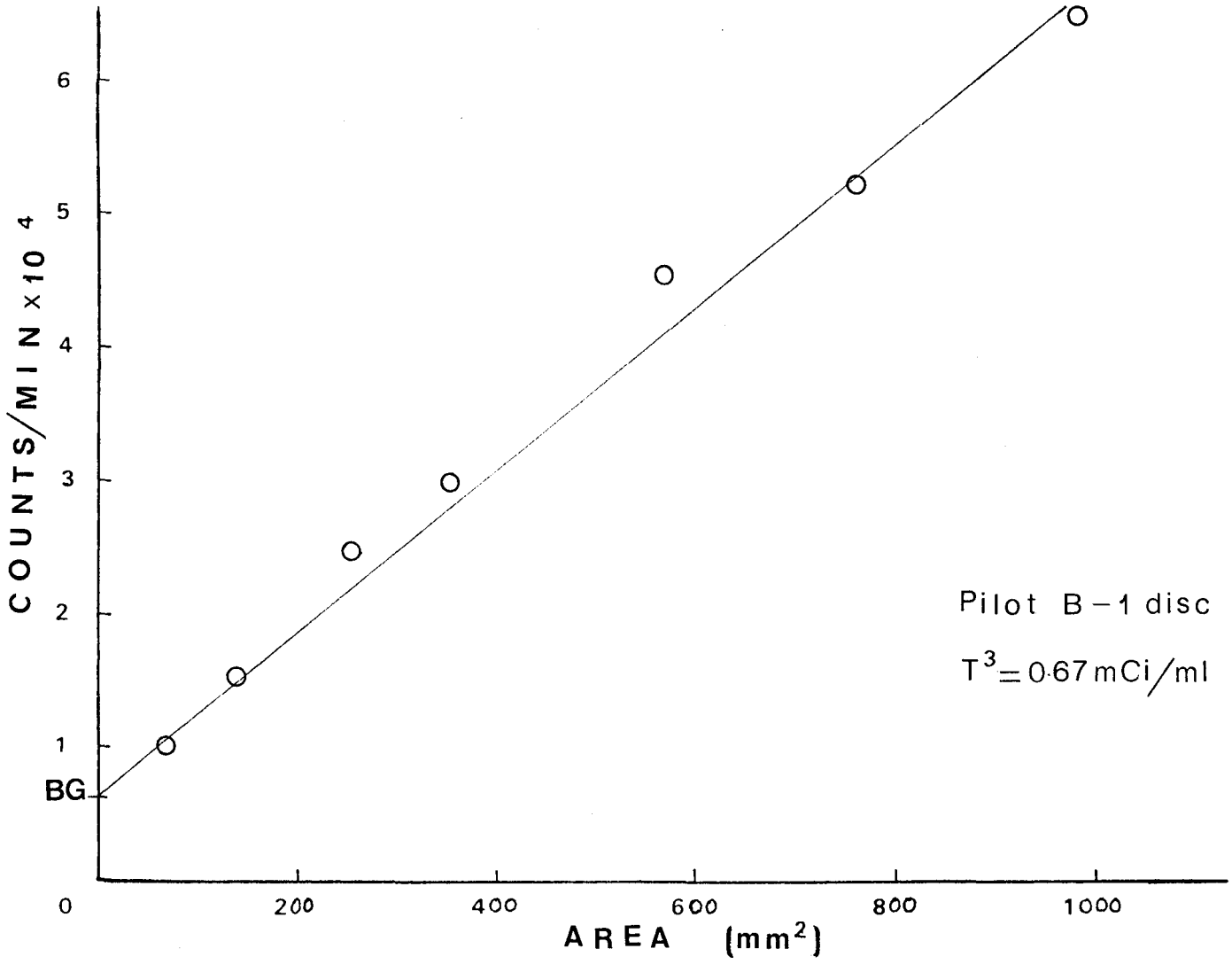

FIG.8. RESPONSE FROM A SINGLE HORIZONTAL DISC

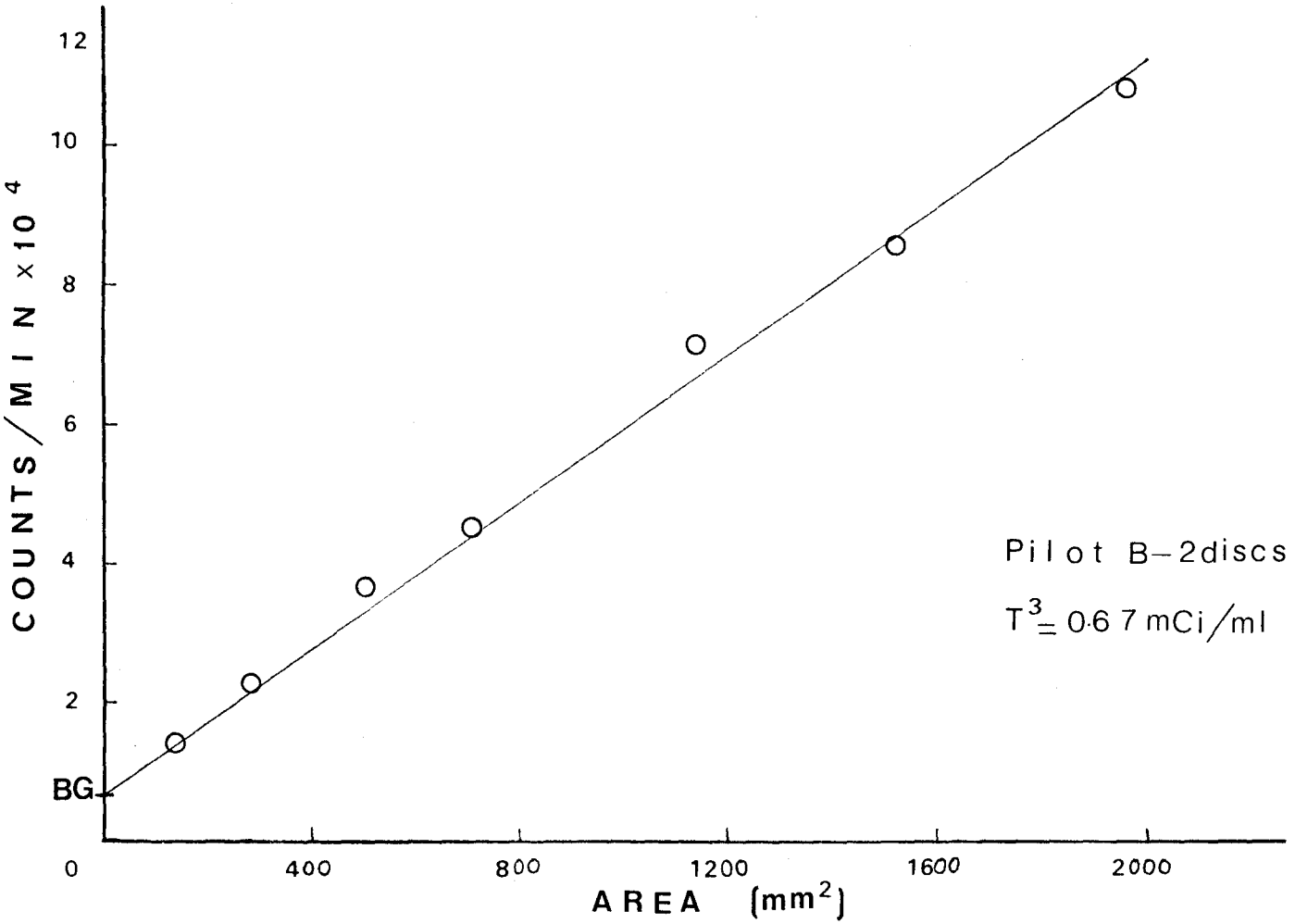

FIG.9. RESPONSE FROM TWO HORIZONTAL DISCS

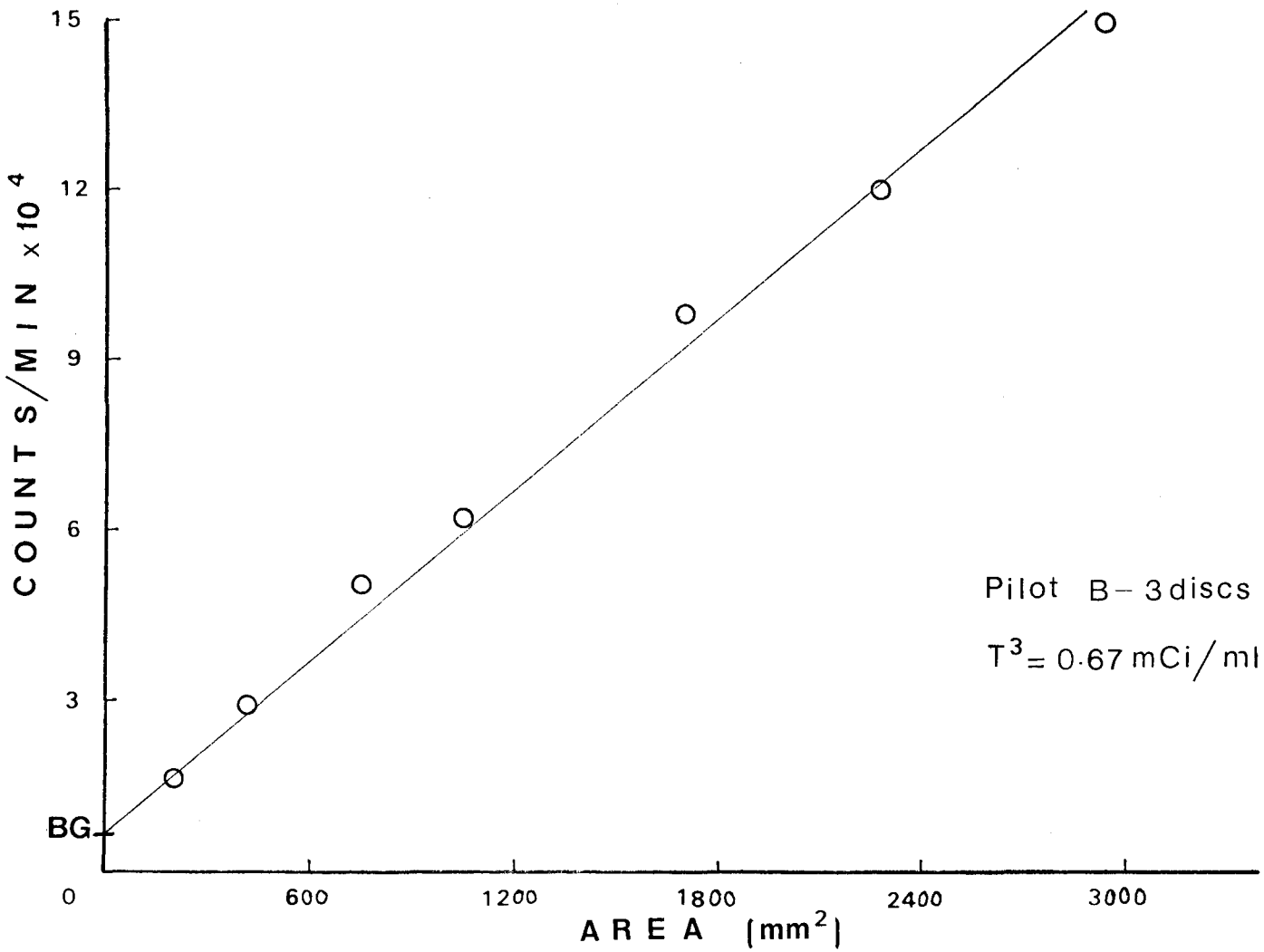

FIG.10. RESPONSE FROM THREE HORIZONTAL DISCS

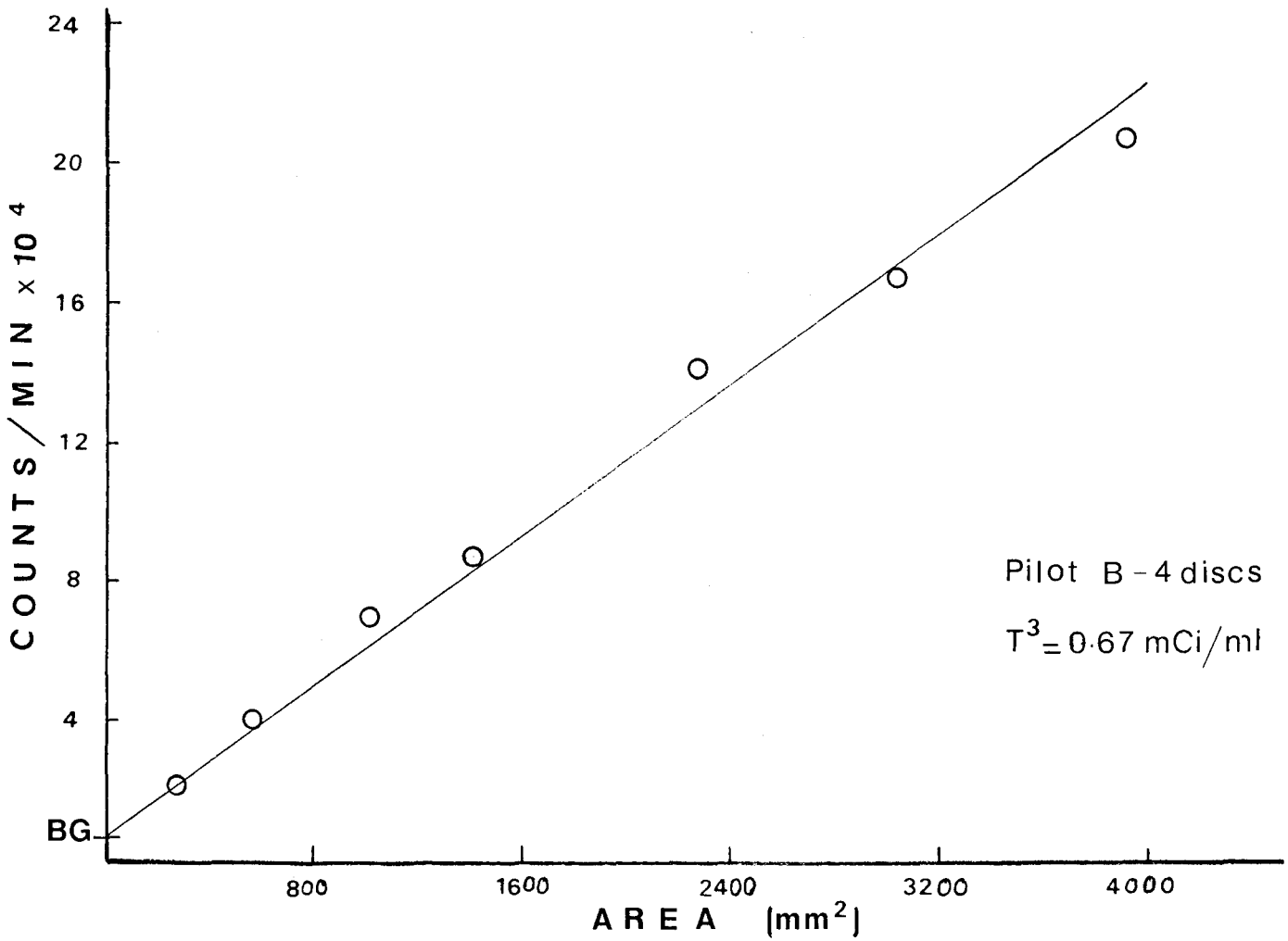

FIG.11. RESPONSE FROM FOUR HORIZONTAL DISCS

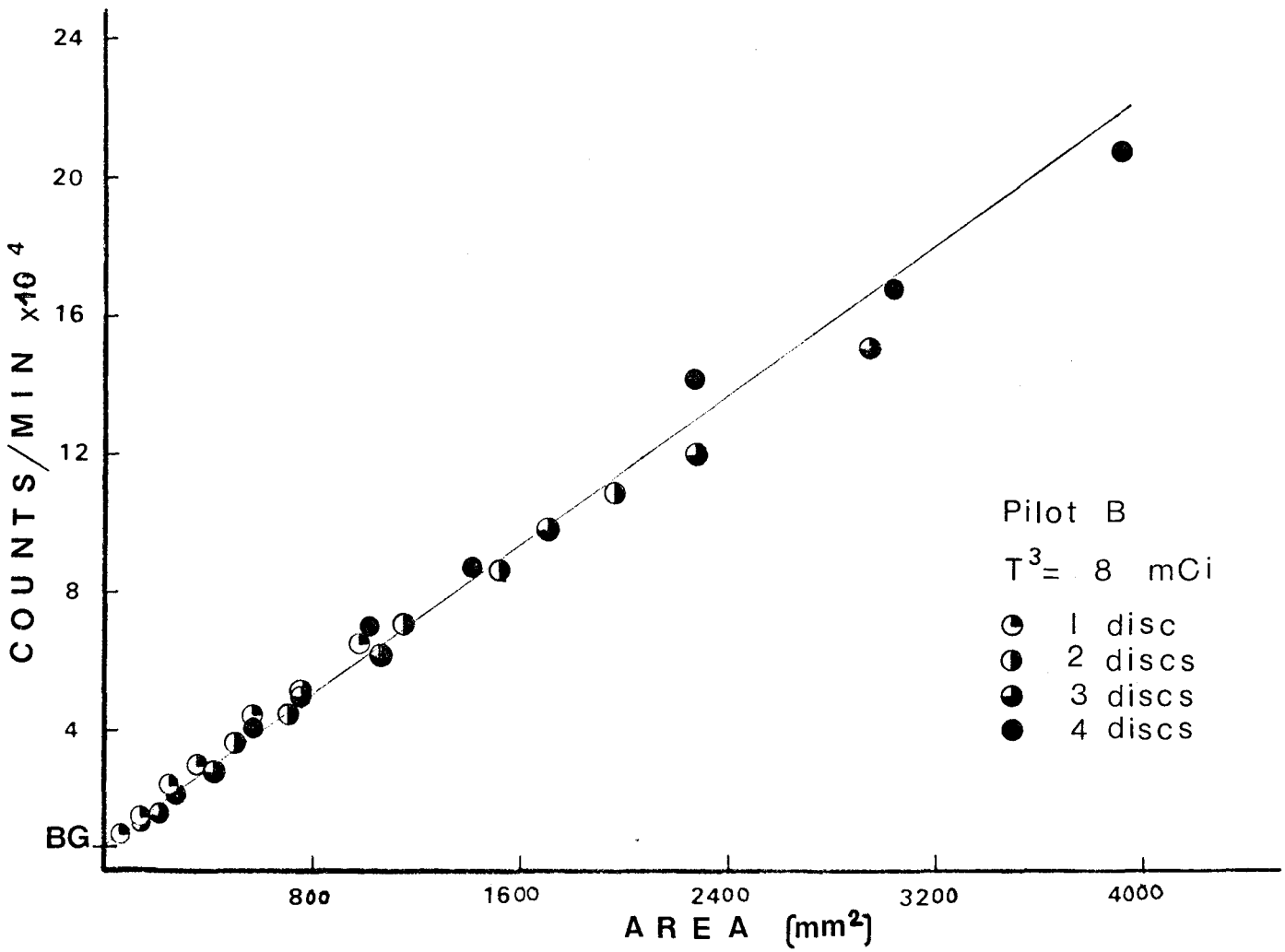

FIG.12. RESPONSE FROM HORIZONTAL DISCS OF DIFFERENT TESTS

of plastic scintillators.

It was observed that a variation in the distance separating scintillator discs did not affect the results. Table 2 shows the results of such test, where the distance was varied from 0.5 to 3 mm. This indicates that the separation distance between two or more discs is irrelevant, and the only thing that matters is the total interfacial area.

Fig. 14 shows schematically the vertical arrangement of the discs. The multiple-disc tests were repeated for this case. Results are shown in Figs. 15-19 and experimental data are tabulated in Table A1.3(II).

TABLE 2: Effect of separation between two scintillator discs on count rate.

Pilot B - 2 discs

Sample volume = 12 mCi

Sample activity = 8 mCi

Counting time = 1 min.

	Background	Distance between the two scintillators (mm)			
		0.5	1	2	3
Counts	7004	82718	85140	83857	88554
	7009	84967	85700	87050	86762
	7359	82611	86466	88621	86593
	8243	82186	86962	86376	87902
	8806	83305	87300	87712	87362
Average Counts	7684	83157	86314	86723	87435

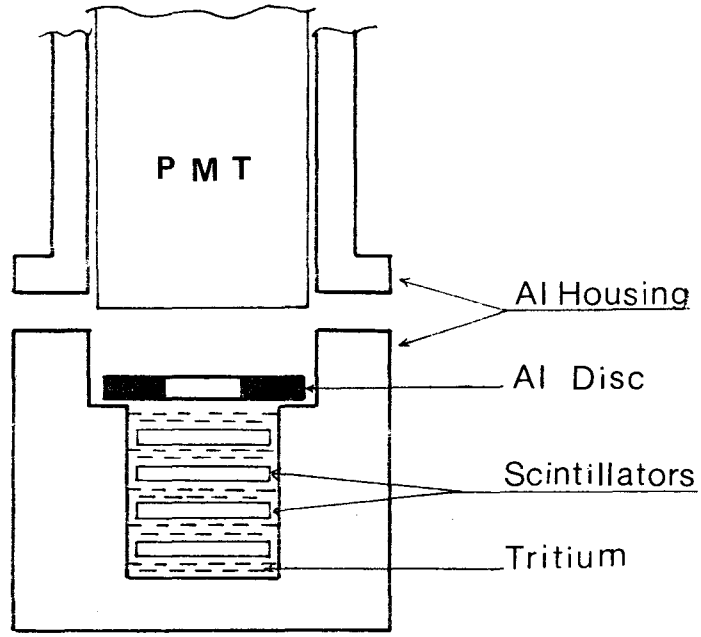

FIG. 13. HORIZONTAL COUNTING ARRANGEMENT

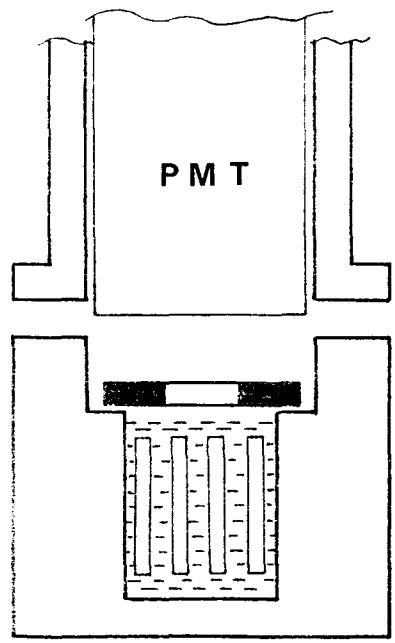

FIG. 14. VERTICAL COUNTING ARRANGEMENT

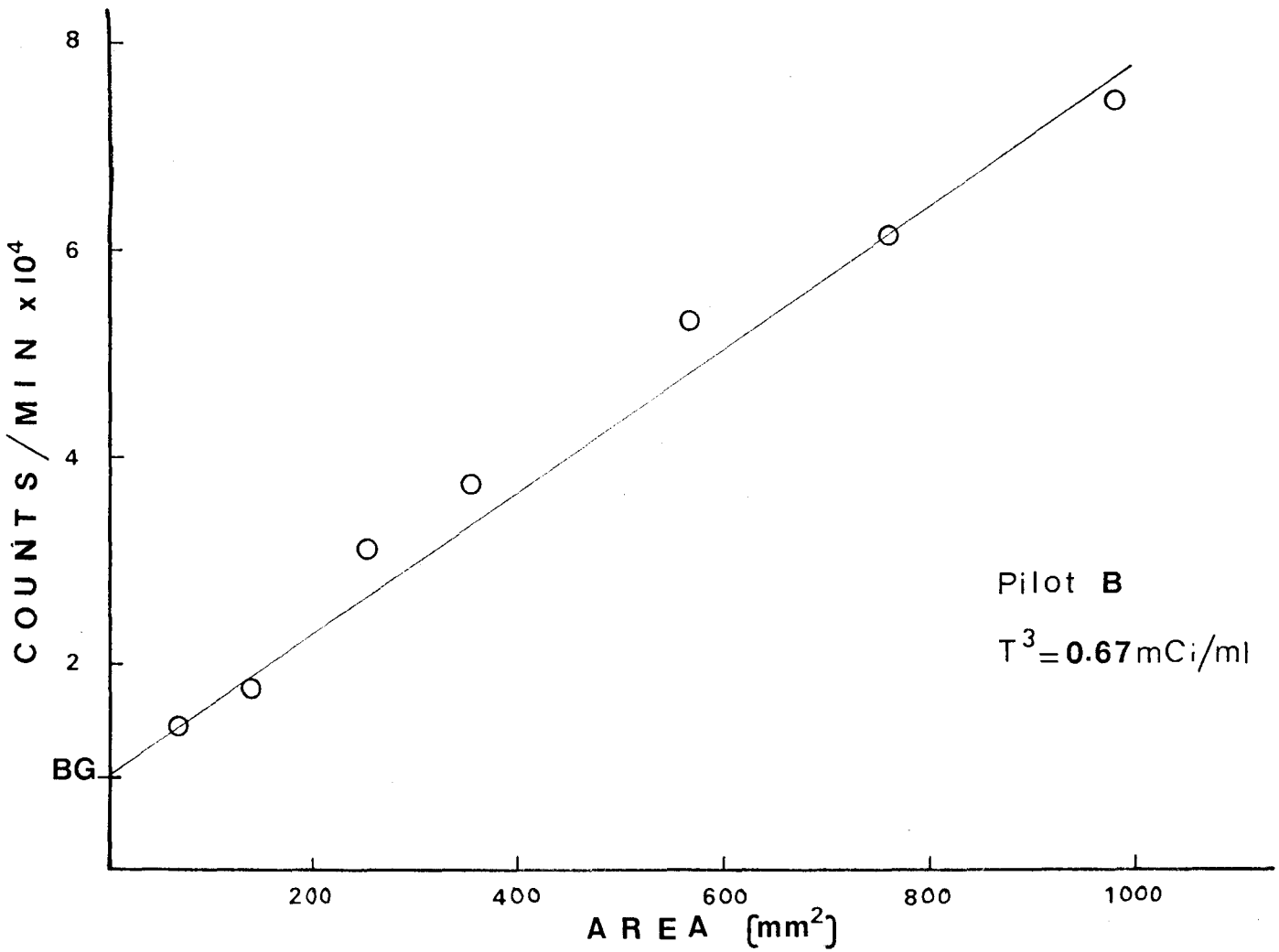

FIG.15. RESPONSE FROM A SINGLE VERTICAL DISC

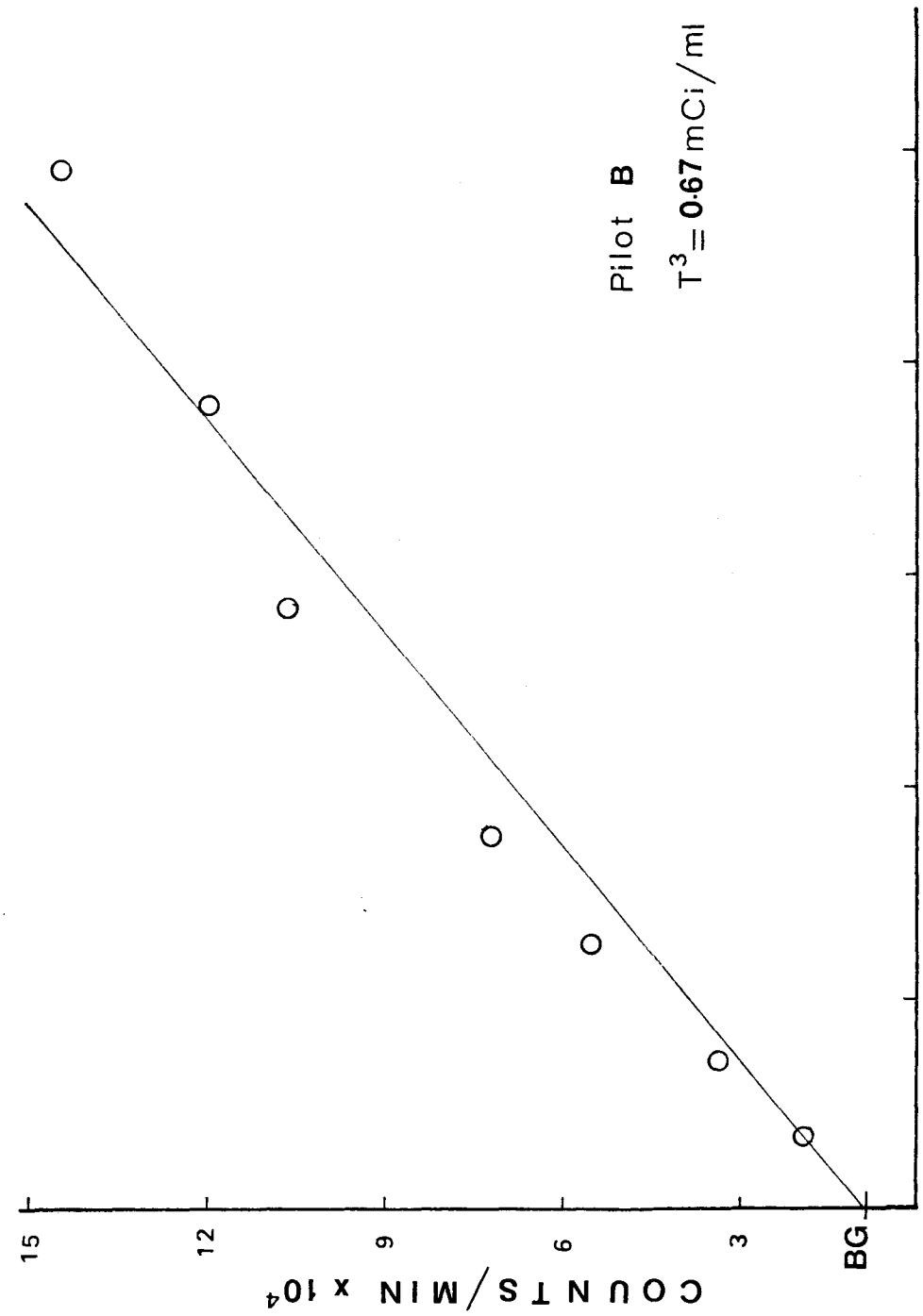

FIG.16. RESPONSE FROM TWO VERTICAL DISCS

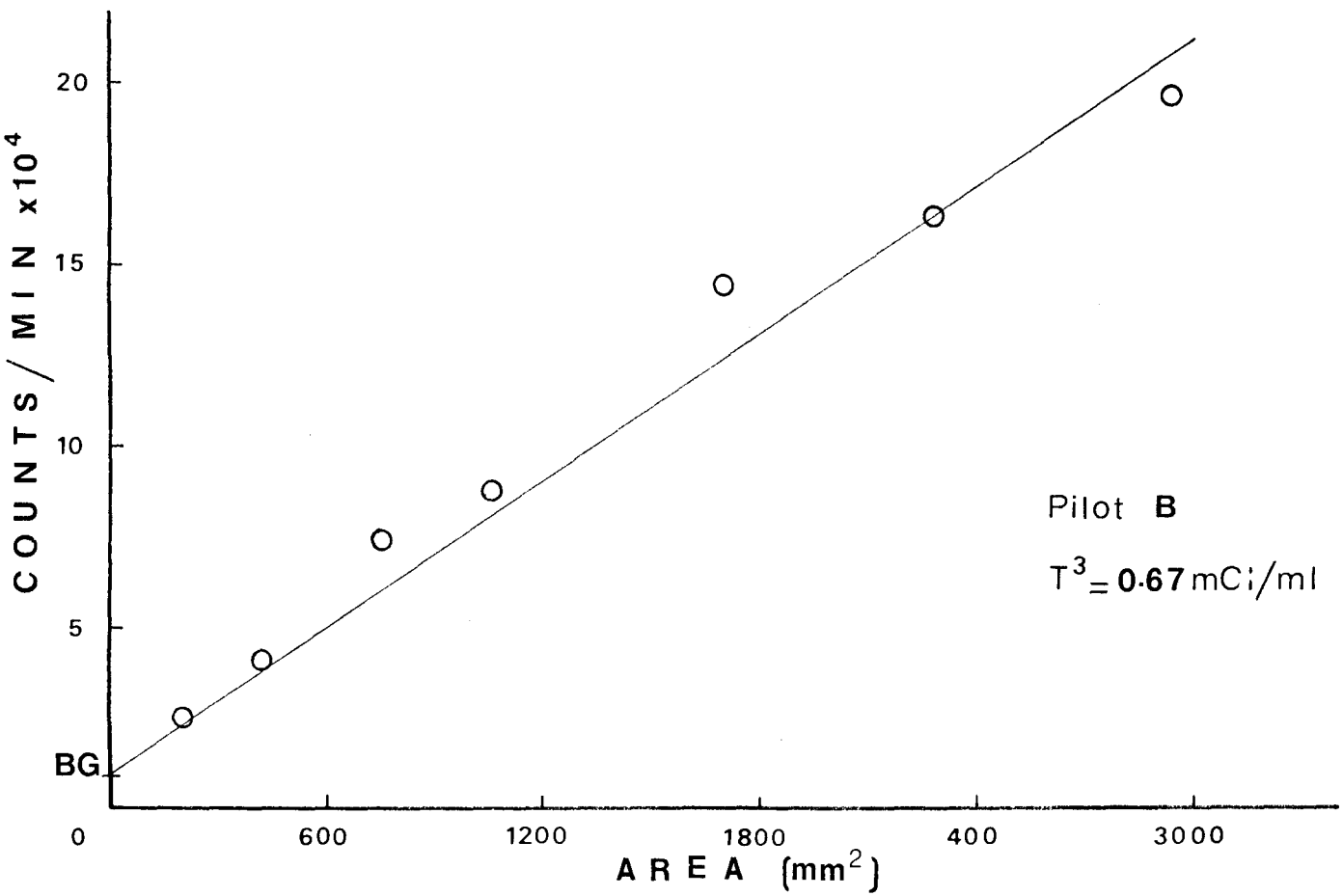

FIG.17. RESPONSE FROM THREE VERTICAL DISCS

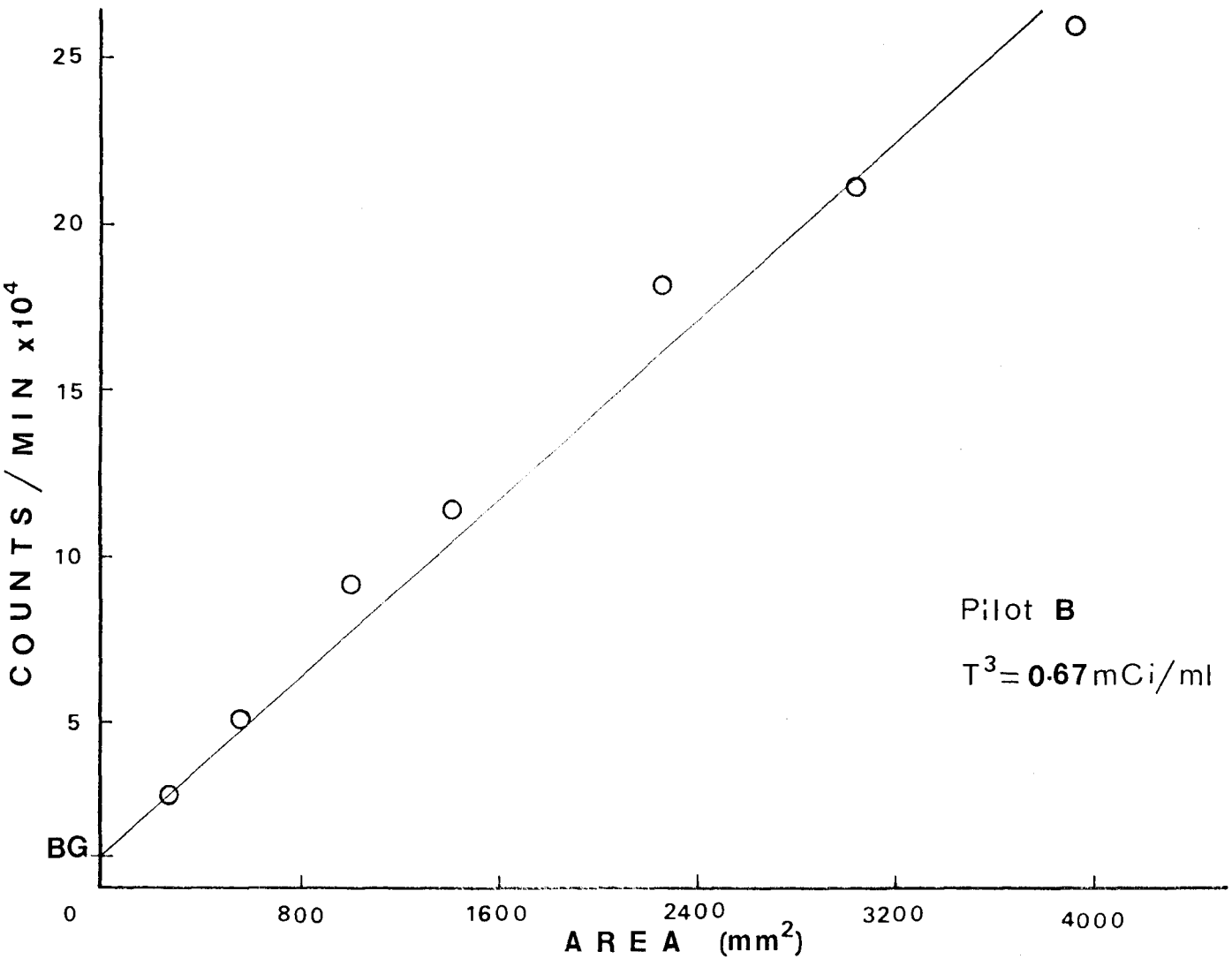

FIG.18. RESPONSE FROM FOUR VERTICAL DISCS

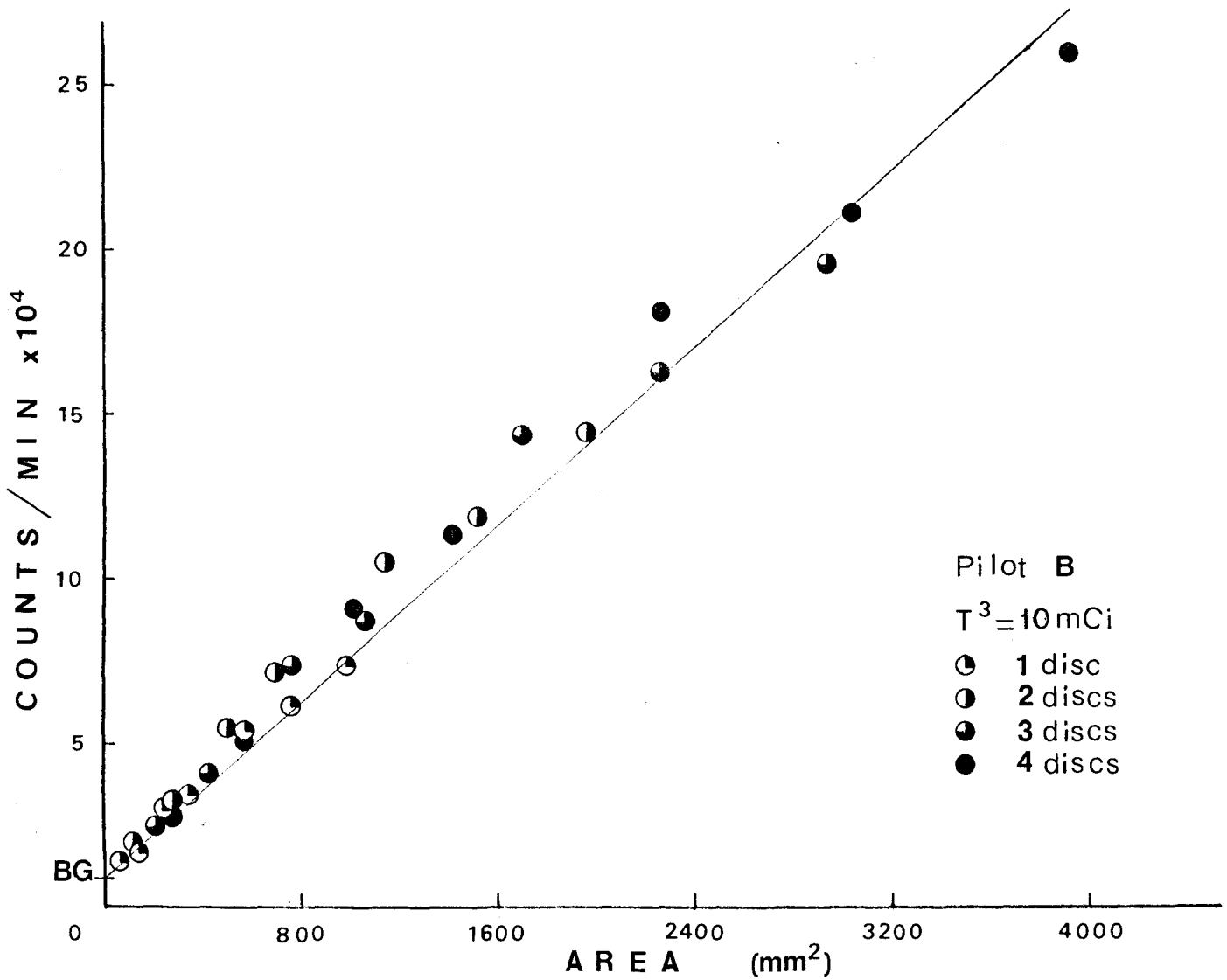

FIG.19. RESPONSE FROM VERTICAL DISCS OF DIFFERENT TESTS

A number of points from the graphs of multiple disc tests (Figs. 12 and 19), were chosen and redrawn on a single graph, Fig. 20. Activity corrections (using Fig. 4), were necessary, since the two tests had different tritium activities, see Table A1.4 and sample calculation A2. It can be deduced that the position of the plastic scintillator whether vertical or horizontal with respect to the PMT, is not significant, and the only thing that should be taken into account is the total interfacial areas.

Results of tests with liquid scintillator NE224 are shown in Figs. 21 and 22. Fig. 21 shows the case where a single container was used. Fig. 22 shows the case when four different diameter containers were used in the two positions; vertical and horizontal. These graphs show that a linear relationship between interfacial area and count rate also exists in the case of the liquid scintillator. However, it was mentioned before that all the four containers had an equal thicknesses of scintillator on top of the tritium. Data for these tests are shown in Table A1.5.

It was observed that the count rate was related to liquid scintillator thickness. So when the thickness was increased the count rate was also increased, as shown in Fig. 23. Similar behaviour was also noticed when using the other liquid scintillator NE213, Fig. 24.

A similar test was arranged with the plastic scintillator discs, using either a single or multiple discs. Results of these tests are shown in Table A1.6 (a, b, c). Variations in readings of plastic scintillator can be seen to be within the statistical error.

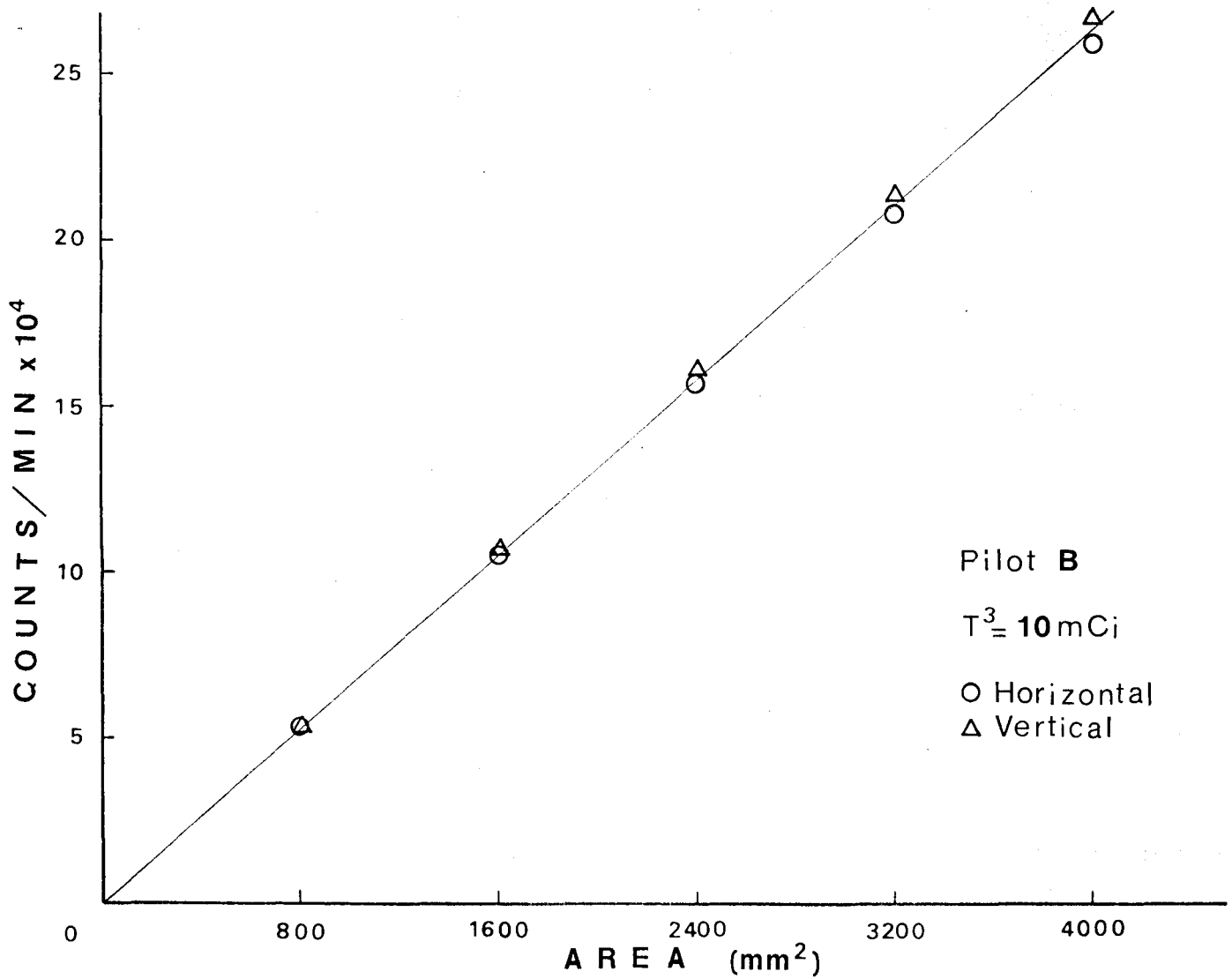

FIG.20. RESPONSE FROM HORIZONTAL AND VERTICAL COUNTING ARRANGEMENTS

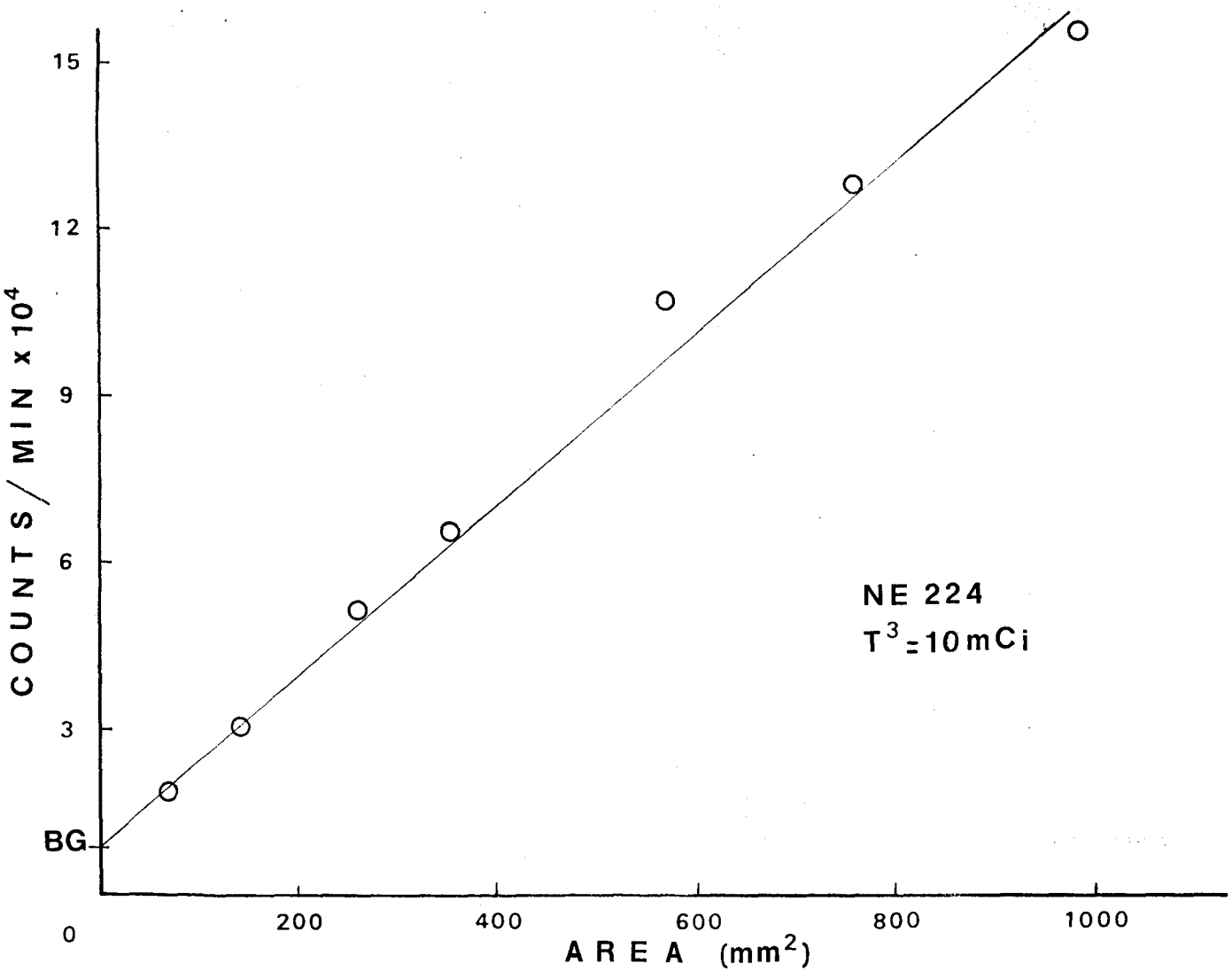

FIG.21. RESPONSE TO LIQUID SCINTILLATOR FROM A SINGLE CONTAINER

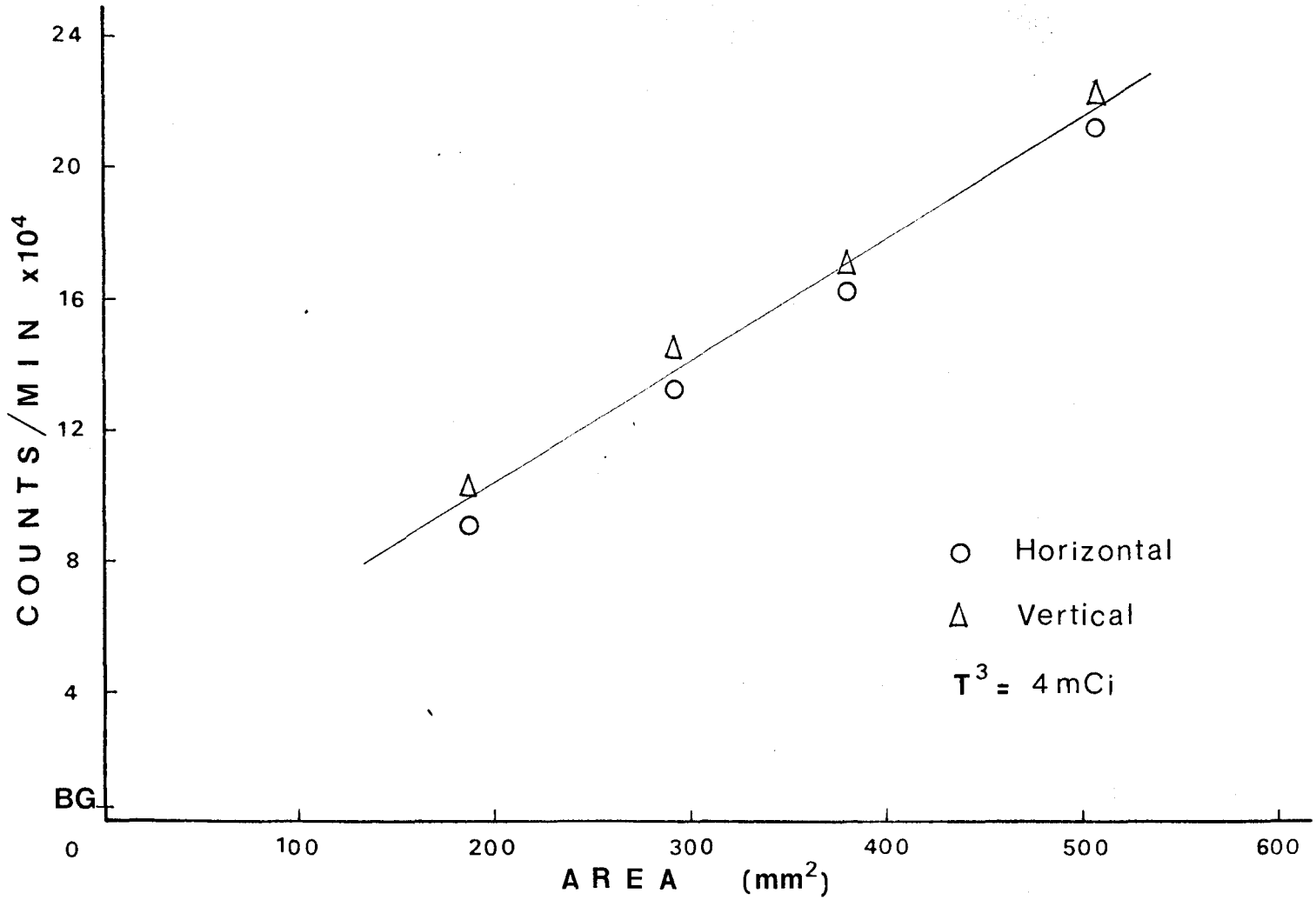

FIG.22. RESPONSE TO LIQUID SCINTILLATOR FROM SEVERAL CONTAINERS

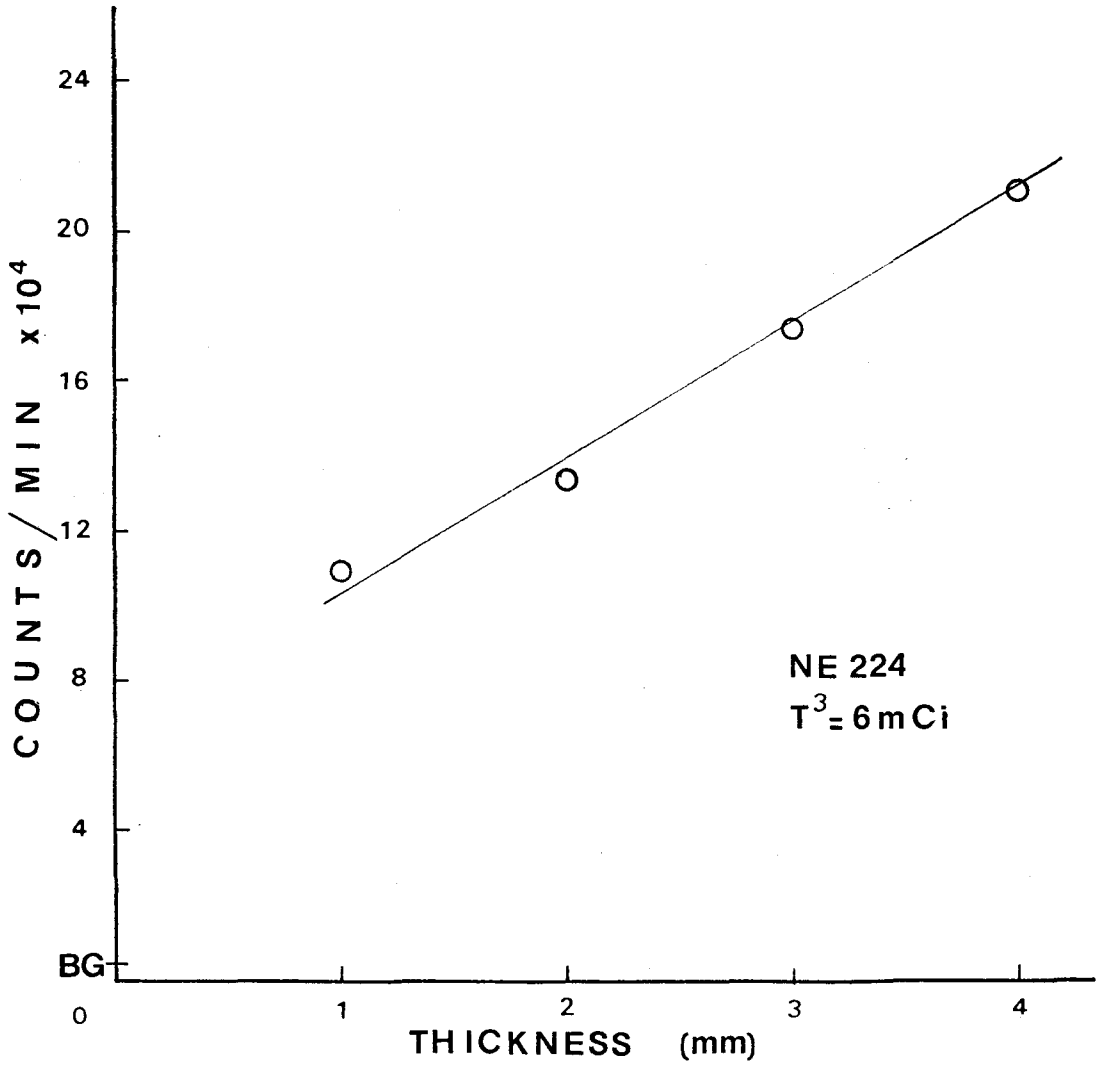

FIG.23. EFFECT OF SCINTILLATOR THICKNESS ON COUNT-RATE

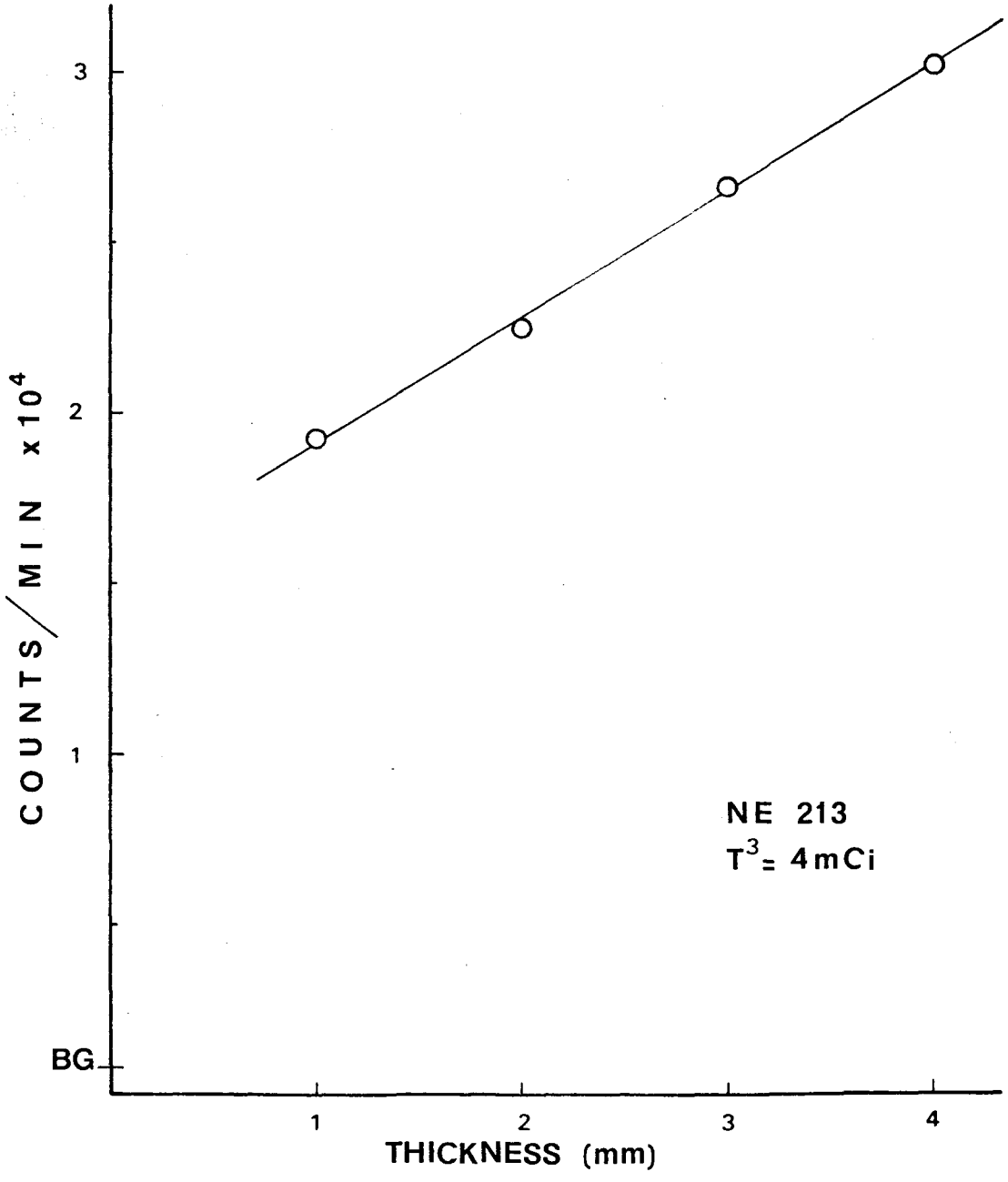

FIG. 24. EFFECT OF SCINTILLATOR THICKNESS ON COUNT RATE

A systematic investigation was done to determine the cause for the anomalous behaviour of the liquid scintillators. The absorption distance of the β-rays is so small that the thickness should have no effect. Therefore it was suggested that the increase in count rate would be due to self fluorescence in the liquid scintillators. To check this a control test was run using distilled water and liquid scintillator only. The thickness of scintillator was varied, but the count rate remained constant, within the experimental error, see Table A1.6(d).

Another test was run with liquid scintillator and distilled water, to see the effect of time elapsed on the count rate. The sample was kept inside the light-tight housing for six hours, and readings were taken every hour interval. No change in the count rate was observed, as shown in Table A1.7(a). Similar effect was noticed with a tritium sample, Table A1.7(b).

No explanation has yet been found for the anomalous behaviour of the liquid scintillators with thickness. The plastic scintillator does not show an increase in count rate with thickness but the liquids do. One possible explanation is that the liquid scintillators may emit a primary photon in an energy range that is not ideal for the photomultiplier tube. To shift the frequency, a secondary solute may have been used, which gives rise to this behaviour.

It is also suggested that the increase in counts is due to the slight solubility of water in the liquid scintillators. As scintillator volume is increased there will be a greater percentage of total tritium sample in the scintillator [37].

5. CONCLUSIONS

A radioactive technique to estimate the interfacial areas between solid-liquid and liquid-liquid phases has been investigated. β-particles from tritium, plastic and liquid scintillators were used in the tests. It was found that a linear relationship exists between interfacial area and count rate, except at very low tritium concentrations, irrespective of the orientation of the scintillators with respect to PMT position. However, anomalous behaviour of the liquid scintillators was observed when the scintillator thickness was varied. The count rate varied with thickness for a fixed interfacial area, although the maximum range of β-particles from tritium is much less than the thickness under investigation. Also, solubility of scintillator in tritium solution is negligible and does not appear to account for the increase. This behaviour was not encountered with the plastic scintillator. More investigation into the chemical composition of the liquid scintillator components is needed to explain this behaviour. In the mean time, one should look into some other types of liquid scintillators or prepare a liquid scintillator which will not show this behaviour.

The technique is simple and non-hazardous. It is hoped that it can be used to study behaviour in two-phase flow, once the anomalous behaviour of the liquid scintillator is explained, because of high sensitivity that radioactive methods offer. One of the phases could be labelled with tritium and liquid scintillator could be used for the second phase. Several PMT may be employed if necessary. Scattering

of lights from a scintillating bubble is not a serious problem, since these can be considered as isotropic sources.

BIBLIOGRAPHY

[1] Sideman, S., Hortacsu, O. and Fulton, J.W., Ind. Engng. Chem., V58, p. 32, 1966.

[2] Valentin, F.H.H., "Absorption in Gas-Liquid Dispersions: Some Aspects of Bubble Technology", E. and F.N. Spon Ltd., London, 1967.

[3] Sharma, M.M. and Danckwerts, P.V., Br. Chem. Engng., V15, p. 522, 1970.

[4] Shilimkan, R.V. and Stepanek, J.B., Chem. Engng. Sci., V32, p. 149, 1977.

[5] Kasturi, G. and Stepanek, J.B., Chem. Engng. Sci., V29, p. 1849, 1974.

[6] Sridharan, K. and Sharma, M.M., Chem. Engng. Sci., V31, p. 767, 1976.

[7] Metha, V.D. and Sharma, M.M., Chem. Engng. Sci., V26, p. 461, 1971.

[8] Westerterp, K.R., Van Dierendonck, L.L. and Kraa, J.A., Chem. Engng. Sci., V18, p. 157, 1963.

[9] Linek, V. and Mayrhoferova, J., Chem. Engng, Sci., V24, p. 481, 1969.

[10] Vermeulen, T., Williams, G.M. and Langlois, G.E., Chem. Engng. Prog., V51, p. 85F, 1955.

[11] Calderbank, P.H., Trans. Instn. Chem. Engrs., V36, p. 443, 1958.

[12] McLaughlin, C.M. and Rushton, J.H., A.I.Ch.E.J., V19, p. 819, 1973.

[13] Curl, R.L., A.I.Ch.E.J., V20, p. 184, 1974.

[14] Lee, J.C. and Meyrick, D.L., Paper presented at the symposium on Gas-Liquid Reactions, Inst. Chem. Engrs., Manchester, January 1969.

[15] Landau, J., Boyle, J., Gomaa, H.G. and Al-Taweel, A.M., Can. J. Chem. Engng., V55, p. 13, 1977.

[16] Calderbank, P.H., Evans, F. and Rennie, J., Proc. Int. Symp. on Dist., Inst. Chem. Engrs., London, 1960.

[17] Van Dierendonck, L.L., Fortuin, J.M.H. and Venderbos, D., Paper presented at the Fourth European Symposium on Chemical Reaction Engineering, Brussels, 1968.

[18] Towell, G.D., Strand, C.P. and Ackerman, G.H., A.I.Ch.E.I. Chem. E., Symposium Series No. 10. Inst. Chem. Engrs., London, 1965.

[19] Kawecki, W., Reith, T., Van Heuven, J.W. and Beek, W.J., Chem. Engng. Sci., V22, p. 1519, 1967.

[20] Brown, D.E. and Craddock, J., Paper presented at the symposium on Mixing, Inst. Chem. Engrs., Leeds, September, 1969.

[21] Reith, T. and Beek, W.J., Paper presented at the Fourth European Symposium on Chemical Reaction Engineering, Brussels, 1968.

[22] Reith, T., Br. Chem. Engng., V15, p. 1559, 1970.

[23] Sridhar, T. and Potter, O.E., Chem. Engng. Sci., V33, p. 1347, 1978.

[24] Horrocks, D.L., "Applications of Liquid Scintillation Counting", Academic Press, N.Y. 1974.

[25] Price, W.J., "Nuclear Radiation Detection", McGraw Hill, 1964.

[26] Attix, F.H. and Roesch, W.C., eds., "Radiation Dosimetery", VII, Academic Press, N.Y. 1966.

[27] Stanley, P.E. and Scoggins, B.A., eds., "Liquid Scintillation Counting, Recent Developments", Academic Press Inc., N.Y. 1974.

[28] Noujaim, A.A., Ediss, C. and Weibe, L.I., eds., "Liquid Scintillation, Science and Technology", Academic Press Inc., N.Y. 1976.

[29] Horrocks, D.L., and Peng, C.T., eds., "Organic Scintillators and Liquid Scintillation Counting", Academic Press, N.Y. 1971.

[30] Lamarsh, J.R., "Introduction to Nuclear Engineering", Addison-Wesley Pub. Co., 1975.

[31] Heitler, W., "The Quantum Theory of Radiation", Oxford Univ. Press, London 1954.

[32] Katz, L. and Penfold, A.S., Revs. Mod. Phys., V24, p. 28, 1952.

[33] Evans, E.A., "Tritium and its Compounds", John Wiley and Sons, N.Y. 1974.

[34] Blincow, D.W. and Webster, J.R., IEEE Trans. Nuc. Sci., NS-11, No. 3, p. 38-43, 1964.

[35] Timmerhaus, K.D., Giller, E.B., Duffied, R.B. and Drickamer, H.G., Nucleonics, V6, p. 37, June 1950.

[36] Monk, G.S., "Light-Principles and Experiments", McGraw Hill, 1937.

[37] Private communications from Nuclear Enterprises, Inc.

APPENDIX

A1. Test Data

TABLE A1.1 Data for Test No. 1

Pilot B

Sample Volume = 2 ml

Counting time = 1 min

Activity (mCi)	Counts	Average Counts
Background	6513, 6470, 6300, 6533, 6240	6411
0.5	58933, 58950, 59602, 59976, 59852	59463
1	64251, 65027, 65878, 66611, 66026	65559
3	117385, 119102, 120661, 121202, 121791	120028
6	208057, 209679, 210860, 212684, 212666	210789
8	266226, 266808, 270342, 272005, 272844	269645
10	348406, 351504, 355380, 355786, 356811	353577
12	412203, 415364, 416001, 418437, 420022	416405
16*	437454, 445564, 449046, 450630, 445660	445690
18**	470170, 471102, 473967, 479242, 481378	475172
20***	530471, 532045, 535254, 542451, 540073	536059

* Dead time = 12%, therefore average count is 499154.

** Dead time = 14%, therefore average count is 541696

*** Dead time = 16%, therefore average count is 621828

TABLE A1.2 Data for Test No. 2

Pilot B

Sample volume = 2 ml

Counting time = 1 min

a. Activity = 0.5 mCi

Area* (mm^2)	Counts	Average Counts
Background	9111, 8028, 7469, 8445, 8923	8395
A_1	10347, 10951, 11197, 11457, 11925	11175
A_2	13811, 15040, 15377, 15051, 15664	14989
A_3	19411, 19014, 19657, 19853, 19150	19417
A_4	21293, 20775, 20859, 20601, 21391	20984
A_5	28190, 29387, 29610, 29628, 30114	29386
A_6	29239, 31830, 33532, 33311, 32808	32144
A_7	35062, 37564, 37673, 37494, 37156	36990

b. Activity = 6 mCi

Area (mm^2)	Counts	Average Counts
Background	6064, 5861, 6200, 6527, 6306	6192
A_1	16580, 16346, 17327, 18456, 18412	17424
A_2	29629, 29776, 29954, 30706, 30233	30060
A_3	49312, 49754, 50746, 50912, 50411	50227
A_4	60945, 61577, 62294, 62914, 63087	62163
A_5	100671, 100921, 100420, 100863, 101986	100972
A_6	113789, 115178, 115239, 115634, 115715	115111
A_7	143392, 143478, 143408, 143192, 143977	143490

c. Activity = 8 mCi

Area (mm^2)	Counts	Average Counts
Background	7024, 7151, 7076, 7117, 7261	7126
A_1	21109, 19303, 19245, 19647, 19812	19823
A_2	28380, 28728, 28947, 29159, 29339	28911
A_3	48738, 49499, 49575, 49910, 50182	49581
A_4	63366, 63609, 65111, 66224, 65773	64817
A_5	104014, 104728, 105562, 106022, 107044	105474
A_6	124082, 125511, 127031, 127815, 127999	126488
A_7	154027, 155814, 155316, 155892, 156444	155499

* see Table A1.8

TABLE A1.3 Data for Test No. 3

Pilot B

I. Horizontal Positions

Sample volume = 12 ml

Sample activity = 8 mCi

Counting time = 1 min

a. Single disc

Area (mm^2)	Counts	Average counts
Background	5127, 5378, 6417, 6732, 6615	6054
A_1	9666, 9699, 9884, 10257, 10639	10029
A_2	15059, 15193, 15232, 15058, 15393	15187
A_3	24212, 24439, 24660, 24644, 25206	24632
A_4	28806, 29346, 29783, 30580, 31285	29960
A_5	44535, 45887, 45129, 46101, 45902	45511
A_6	51975, 52483, 52350, 52018, 52658	52297
A_7	63026, 65426, 65009, 65473, 65369	64861

b. Two discs

Area (mm^2)	Counts	Average counts
Background	5756, 6116, 6070, 6740, 8460	6628
A_1	13035, 14790, 14933, 13769, 14077	14121
A_2	21500, 21818, 22176, 22454, 25290	22648
A_3	37583, 37025, 36361, 36481, 36368	36764
A_4	44425, 44912, 44646, 45118, 46290	45078
A_5	69799, 71216, 71205, 71610, 71402	71046
A_6	84747, 84627, 86717, 87714, 87220	86205
A_7	104928, 107948, 108781, 109393, 109967	108203

c. Three discs

Area (mm^2)	Counts	Average Counts
Background	5756, 6116, 6070, 6740, 8460	6628
A_1	16283, 16543, 16417, 16260, 16509	16402
A_2	28879, 29563, 29259, 29676, 30023	29480
A_3	49870, 50993, 50167, 51028, 50203	50452
A_4	61588, 62085, 61804, 62348, 62686	62102
A_5	98562, 98284, 98378, 98852, 98790	98573
A_6	120489, 119158, 120235, 120528, 120442	120170
A_7	145435, 150091, 151177, 150398, 151318	149684

d. Four discs

Area (mm^2)	Counts	Average Counts
Background	5756, 6116, 6070, 6740, 8460	6628
A_1	21637, 21731, 21919, 21723, 21883	21779
A_2	40155, 40127, 40737, 40576, 40601	40439
A_3	69473, 69554, 69671, 69377, 69491	69513
A_4	86246, 86066, 86571, 88361, 88560	87161
A_5	141769, 141069, 141773, 141846, 141631	141618
A_6	165824, 166797, 167068, 167893, 167932	167103
A_7	207605, 207574, 207947, 207952, 207768	207770

II. Vertical Positions

Sample volume = 15 ml

Sample activity = 10 mCi

Counting time = 1 min

a. Single disc

Area (mm^2)	Counts	Average Counts
Background	7505, 8436, 9225, 11323, 8729	9044
A_1	14023, 14053, 14743, 13524, 14309	14130
A_2	18451, 18124, 15262, 15233, 20680	17550
A_3	30728, 31221, 29503, 32180, 32511	31229
A_4	37504, 36425, 36212, 39047, 37887	37415
A_5	51321, 51816, 53029, 55225, 53824	53043
A_6	58737, 61749, 61586, 61440, 63634	61429
A_7	72818, 72622, 74623, 76148, 74671	74176

b. Two discs

Area (mm^2)	Counts	Average Counts
Background	7505, 8436, 9225, 11323, 8729	9044
A_1	19024, 19277, 19086, 18910, 18982	19056
A_2	33531, 33543, 33358, 33529, 33629	33518
A_3	55173, 55561, 54843, 55257, 55113	55189
A_4	69966, 72704, 72746, 71768, 73269	72091
A_5	106052, 106823, 105820, 106624, 106586	106381
A_6	120228, 119413, 120749, 119172, 117280	119368
A_7	140061, 143442, 145267, 144625, 147554	144190

c. Three discs

Area (mm^2)	Counts	Average Counts
Background	7505, 8436, 9225, 11323, 8729	9044
A_1	24420, 25068, 25553, 26071, 24588	25140
A_2	43843, 45304, 37507, 37951, 38289	40579
A_3	70038, 74628, 75026, 75135, 74862	73938
A_4	85507, 85322, 85906, 89127, 93054	92783
A_5	146548, 144360, 145148, 143975, 141055	144217
A_6	163629, 162516, 162963, 162727, 163435	163054
A_7	195487, 195716, 194923, 195661, 196256	195609

d. Four discs

Area (mm^2)	Counts	Average Counts
Background	10855, 10725, 10700, 10829, 10745	10771
A_1	27583, 28684, 28263, 27338, 27176	27809
A_2	50445, 50369, 50523, 51124, 51639	50820
A_3	89549, 90818, 92064, 90766, 92224	91084
A_4	113247, 113885, 111227, 112803, 114883	113209
A_5	181269, 182314, 180420, 182051, 181509	181513
A_6	208032, 210805, 211428, 212073, 209069	210281
A_7	255607, 259384, 257531, 257924, 263007	258691

TABLE A1.4 Data for Fig. 20

Interfacial Area (mm^2)	Counts/min		
	Vertical Position Activity 10 mCi (Fig. 19)	Horizontal Position	
		Activity 8 mCi (Fig. 12)	Corrected to 10 mCi (factor = 1.2, Fig. 4)
800	63000	50000	60000
1600	116500	92000	110400
2400	170000	135500	162600
3200	223000	178000	213600
4000	276000	221000	265200

TABLE A1.5 Data for Test No. 5

Liquid scintillator NE 224

a. Single container

Tritium volume = 2 ml

Tritium activity = 10 mCi

Area (mm^2)	Counts	Average counts
Background	7505, 8436, 9225, 11323, 8729	9044
A_1	17508, 19116, 19728, 18406, 19910	18934
A_2	29148, 30342, 30808, 31364, 32086	30750
A_3	4924, 50360, 52708, 51942, 52556	51363
A_4	64668, 66286, 66540, 65680, 65472	65729
A_5	104726, 103436, 109248, 108846, 108040	106860
A_6	127848, 125774, 129710, 129480, 127778	127718
A_7	154510, 154158, 154712, 157322, 156298	155400

b. Four containers

Tritium volume = 2 ml

Tritium activity = 4 mCi

I. Position when PMT and container axes are in-line

* See Table A1.8

	Background	Interfacial Area* (mm^2)			
		S_1	S_2	S_3	S_4
Counts	5049 5625 5496 4796 5108	102805 102761 102189 102720 102075	146074 144627 142978 143333 142716	166893 169257 170178 169960 172108	223143 223922 221808 221862 221741
Average Counts	5215	102510	143946	169679	222495

II. Position when PMT and container axes are at right-angle

	Background	Interfacial Area (mm^2)			
		S_1	S_2	S_3	S_4
Counts	5177	92326	132295	162216	213042
	4670	90344	131808	161187	212592
	5385	90377	131821	161628	211730
	5196	90582	132991	163413	211056
	5485	89334	132723	164303	212274
Average counts	5183	90593	132328	162549	212139

TABLE A1.6 Data for Test No. 6

Effect of Scintillator Thicknesses

a. Plastic Scintillator

Sample volume = 2ml

Sample activity = 6 mCi

	Background	Scintillator Thickness (mm)					
		2	3	4.5	6	7.5	10.5
Counts	4466 4399 4698 4399 4157	28091 29046 29093 29257 28687	26776 28150 28672 31678 32019	32505 34178 34601 34152 34459	33761 35475 34795 34141 35703	36310 37751 38622 39207 38572	38262 34801 43777 42827 46255
Average Counts	4424	28835	29459	33979	34775	38092	42984

b. Liquid scintillation NE 224

Sample volume = 2 ml

Sample activity = 6 mCi

	Background	Scintillator Thickness (mm)			
		1	2	3	4
Counts	4670 5385 5196 5485 5177 5049 5625 5496 4796 5108	107132 107905 108834 109173 109398 109776 110005 109402 110215 110208	130716 130708 130204 131423 133717 132992 134690 134244 135539 135887	171159 169867 170221 170695 171809 173001 173521 174747 175722 177226	210440 208751 209221 208745 209320 209218 210818 210755 210944 212092
Average Counts	5199	109205	133012	172797	210030

Table A1.7 Data for Test No. 7

Effect of time on a scintillating sample

a.

Liquid scintillator NE 224

Volume of inactive distilled water = 2 ml

Thickness of scintillator above water surface = 3 mm

	Time Elapsed (hrs.)						
	0	1	2	3	4	5	6
counts/min	9322	10547	9887	10005	10029	9478	9429
	10060	10791	9663	9439	9665	9977	10387
	10676	10669	9308	9669	9991	10101	10501
	10447	10445	9330	9709	10706	10345	10648
	12013	10419	9209	9577	10704	10804	10609
	11846	10315	8857	9731	10710	10066	11459
	11568	10520	9025	9340	10666	9895	12585
	11942	10687	8974	9251	10318	9339	12233
	12480	10474	8878	9387	10320	9654	12014
	12818	10617	9074	9649	10513	10376	11206
Average counts/min	11317	10548	9221	9576	10362	10004	11107

b.

Liquid scintillator NE 224

Volume of tritium sample = 2 ml

Activity of tritium = 6 mCi

Thickness of scintillator above tritium surface = 4 mm

c. Liquid Scintillator NE 213

Sample volume = 2 ml

Sample activity = 4 mCi

	Background	Scintillator Thickness (mm)			
		1	2	3	4
Counts	779 762 740 854 828 818 692 752 792 795	19724 19132 19463 19062 19129 19118 19620 19170 19287 19002	23889 23648 23773 23519 23444 23290 23465 23698 23538 23434	26482 26335 26479 26324 26728 26677 26771 26850 26681 26588	30323 30587 30407 29975 30418 30261 29933 29810 30206 30058
Average Counts	781	19271	23570	26592	30198

d. Liquid Scintillator NE 224

Inactive distilled water volume = 2 ml

	Scintillation Thickness (mm)		
	0.53	1.60	2.63
Counts	4667 5666 5059 4247 4148	4453 4552 4183 3937 4298	4199 4468 4486 4625 5542
Average Counts	4757	4285	4664

	Time Elapsed (hrs.)			
	0	1.25	19.75	21.75
Counts/min	144508	163700	162702	161598
	153755	164481	162979	160495
	154500	165178	161424	161168
	157060	163760	161560	159619
	159688	164812	160923	159846
Average counts/min	153902	164386	161918	160545

TABLE A1.8 Magnitudes of interfacial areas

Symbol	Aluminum Discs	
	Hole diameter (mm)	Hole area (mm^2)*
A_1	6.75	35.75
A_2	9.53	71.26
A_3	12.70	126.68
A_4	15.0	176.75
A_5	19.05	285.02
A_6	22.0	380.13
A_7	25.0	490.87

* Above values are for one face only

TABLE A1.9 Plexiglas containers dimensions used in liquid scintillation counting

Symbol	Plexiglas containers			
	Outside Dia. (mm)	Inside Dia. (mm)	Wall thickness (mm)	Inner x-sec. Area (mm^2)
S_1	17.44	15.44	1	187.23
S_2	21.3	19.3	1	292.55
S_3	24.0	22.0	1	380.13
S_4	27.4	25.4	1	506.71

A2. Sample Calculation

A sample calculation is given here to illustrate the data obtained in Table A1.4 to plot Fig. 20. Two tests were involved in this, where sample activities differed from one to another.

In this calculation, we are interested in Figs. 4, 12 and 19. Fig. 19 used sample activity 10 mCi, whereas Fig. 12 used 8 mCi. Therefore, corrections were necessary so that both figures represent counts from equal activity sample.

e.g. From Fig. 19, interfacial area 800 mm^2 corresponds to 63000 c/min,

From Fig. 12, interfacial area 800 mm^2 corresponds to 50000 c/min,

From Fig. 4, ratio of count rates 10 mCi to 8 mCi = $\frac{325}{270}$ = 1.2

$\therefore$ Corrected count rate to 10 mCi = 50000 x 1.2

= 60000 c/min.

A3. Error Analysis

In general for any counting system, the number of counts registered will be less than the number of radiations emitted by the radioactive source. For a simple counting arrangement, some obvious factors relating to this difference are the geometry of the system, the efficiency of the detector, absorption in source, in air, scattering, etc. and random errors.

A3.1. Statistical Errors

The assumption can be made that results of an experiment subject to random error, if repeated sufficiently often, will average out to the 'true' results of an ideal experiment not subject to random errors. Most of the actual results will be close and very small number quite far

away. This observation leads to the concept of "distribution function" for an experimental measurement subject to random errors. The distribution function is one which describes the fraction of times in large number of measurements that a measurement falls between two specified values.

The average value of a sampling of data is defined as

$$\bar{n} = \frac{1}{N} \sum_{i=1}^{N} n_i$$

where $\bar{n}$ = arithmetic average of count rate

N = number of measurements

n_i = count rate of ith measurement

Error due to statistical fluctuations is given by the square root of the count rate. Standard deviation, which is defined as the square root of the average value of the squares of the individual deviation from the true mean, taken for a large number of observation, was taken as the error due to the count rate, given by

$$\sigma = \left[\frac{1}{N-1} \sum_{i=1}^{N} (\bar{n}-n_i)^2\right]^{1/2}$$

For example, in Test No. 1 for 1 mCi sample, the average count rate is given as

$$\bar{n} = \frac{1}{5} (64251 + 65027 + 65878 + 66611 + 66026)$$

$$= 65559 \text{ counts/min}$$

Error due to statistical fluctuations (1 standard deviation), is

$$\sigma = \left[\frac{1}{5-1}\{(65559 - 64251)^2 + (65559 - 65027)^2 + ...\}\right]^{1/2}$$

$$= 925 \text{ counts/min}$$

$\therefore$ Count rate is 65559 $\pm$ 925 counts/min

A3.2. Error in Plastic Scintillator Area

In calculating the interfacial area of the plastic scintillator, only the two faces of the discs were taken into account. Area due to thickness of the disc was neglected, mainly because this area could not be polished properly with the available equipment, and that the thicknesses were small. The light emitted from this part of the discs would be inefficient compared to the polished surfaces of the discs. However, this would introduce some error, causing a slightly higher count rate than it should actually be.

Assuming that all the surfaces of the disc are polished, then its total surface area S_t is given as

$$S_t = (\pi r^2 \times 2) + (2\pi r \times t)$$
$$= 2\pi r^2 \left(1 + \frac{t}{r}\right)$$

where r is the radius of the disc and t its thickness. The second term of the above expression is the error not accounted for.

If S is the area due to two faces of the disc, then

$$S = 2\pi r^2$$

$$\therefore \text{Percent error} = \frac{S_t - S}{S}$$

$$= \frac{S_t}{S} - 1$$

$$= \frac{t}{r}$$

Since r is constant, then the error is directly proportional to the thickness of the disc as expected. The thiner the disc the less the error.

For r = 25.4 mm

and t = 2 mm

Error = 7.87%

This is the maximum error (for t = 2 mm), assuming that all the surfaces of the disc are polished. Since this is not the case, and only the two faces are polished, then the actual error will be much less than the above value depending on surface conditions of the unpolished parts.

A4. Equipment Specifications

1.	Multi-channel Analyzer:	Type TN-1705
		1024 channels
		CRT display 6.5 ins.
		Integrator
2.	Amplifier:	NA-17
3.	H.V. Power Supply:	NV-25A and TC-909
4.	Preamplifier:	NB-25A
5.	Photomultiplier Base:	Ortec-Model 226
		H.V. Posetive 2.5 kV max.
6.	PMT:	Type XP-1000 (Philips)
		10 stage
		Photocathode dia. = 44 mm
		Max. spectral sensitivity at 400 ± 30 nm
		Anode dark current < 30 nA
7.	Scintillators:	Plastic-Pilot B
		Liquid-NE 224
		Liquid-NE 213
8.	Radioactive source:	Tritium (aqueous)